Chapter 17

Chlorophyll Catabolites and the Biochemistry of Chlorophyll Breakdown

Bernhard Kräutler
Institute of Organic Chemistry, University of Innsbruck, Innrain 52a, A-6020 Innsbruck, Austria

Stefan Hörtensteiner
Institute of Plant Sciences, University of Bern, Altenbergrain 21, CH-3013 Bern, Switzerland

Summary

Although chlorophyll synthesis in Spring and its degradation in Autumn are undoubtedly the most colorful manifestations of life on Earth, chlorophyll catabolism remained an enigma until about fifteen years ago. Contrary to expectation, chlorophyll breakdown in vascular plants rapidly leads to colorless degradation products and only fleetingly involves colored intermediates, which result from enzymatic oxidative opening of the chlorophyll macrocycle. This key oxygenolytic step in higher plants is rapidly followed by an enzymatic reduction to form short-lived fluorescent catabolites. These latter tetrapyrroles isomerize rapidly in an acid-catalyzed chemical step to colorless tetrapyrrolic catabolites. The colorless and non-fluorescent bilanones finally accumulate in the vacuoles of the degreened plant tissues. This chapter outlines the structural features of chlorophyll catabolites from natural sources and the biochemistry of chlorophyll breakdown.

*Author for correspondence, email: bernhard.kraeutler@uibk.ac.at

Bernhard Grimm, Robert J. Porra, Wolfhart Rüdiger and Hugo Scheer (eds): Chlorophylls and Bacteriochlorophylls: Biochemistry, Biophysics, Functions and Applications, pp. 237–260.

I. Introduction

Only in the last fifteen years has chlorophyll (Chl) catabolism in plants begun to yield some of its mysteries (Kräutler et al., 1991; Matile et al., 1996). The earlier lack of knowledge (Brown et al., 1991) is surprising, considering man's fascination with the seasonal appearance and disappearance of the green plant pigments and the emergence of autumnal colors which are probably the most visual signs of life on Earth, observable even from outer space. Chl metabolism is also of obvious ecological and economic importance. More than 10^9 tons of Chl are biosynthesized and degraded every year on earth (Hendry et al., 1987).

This lack of information on the fate of the green plant pigments (Hendry et al., 1987) contrasts with the extensive literature on Chl biosynthesis (Beale and Weinstein, 1991; Chapters 10–15). In this chapter, we review our present knowledge on the structures and reactivity of known Chl catabolites in higher plants, microorganisms and from synthetic sources, as well as the catabolic pathway leading to their formation from the plant Chls. Some of this work has been described in recent reviews (Hörtensteiner, 1999; Kräutler and Matile, 1999; Hörtensteiner and Kräutler, 2000; Kräutler, 2003).

Earlier research failed to detect Chl breakdown products which would permit an informed glimpse at the biological degradative pathway. This earlier search for Chl catabolites was generally directed at finding colored compounds (Matile, 1987), but the major Chl catabolites from vascular plants are now known to be colorless (Kräutler et al., 1991; Matile et al., 1996; Kräutler and Matile, 1999). By analogy to heme breakdown in plants and animals, an oxygenolytic opening of the porphinoid macrocycle was commonly considered as the key step in Chl breakdown (Brown et al., 1991). However, based on the reactivity of chlorins towards electrophilic agents (Woodward and Skaric, 1961), it was assumed that the Chl macrocycle would open at the 'western' C20 meso position (next to the peripherally reduced ring D of the macrocycle, see Scheme 1), where photooxygenolysis of chlorins was also found to occur (Brown et al., 1991); further, Kishi and coworkers (Nakamura et al., 1988, 1989) found that luciferin from the dinoflagellate *Pyrocystis lunula* and a luminescent compound from krill (see Scheme 14, Section IV) were linear tetrapyrroles derived from Chls by cleavage of the macrocycle at C20. Nonetheless, as shown later, macrocycle opening in the major Chl degradative pathway in plants occurs at the 'northern' C5 bridge carbon. For the numbering of the macrocycle, see Scheme 2 and Chapter 1 (Scheer).

Matile et al. (1987) and Thomas et al. (1989) provided the first evidence of non-green Chl catabolites in extracts of senescent leaves of a non-yellowing genotype of the grass *Festuca* (*F.*) *pratensis.* When such extracts were analyzed by chromatography on silica-gel plates and compared with extracts from the naturally degreening wild-type, 'pink' and 'rusty' pigments were formed on the plates but only from extracts of the senescent (degreened) wild-type leaves. These pigments were thought to be artifactual chemical degradation products of the natural colorless catabolites. Similar pigments were formed in yellowing primary leaves of barley (Matile et al., 1988; Bortlik et al., 1990) when forced to degreen in permanent darkness; surprisingly, they were found in the vacuoles rather than in the de-greened chloroplasts

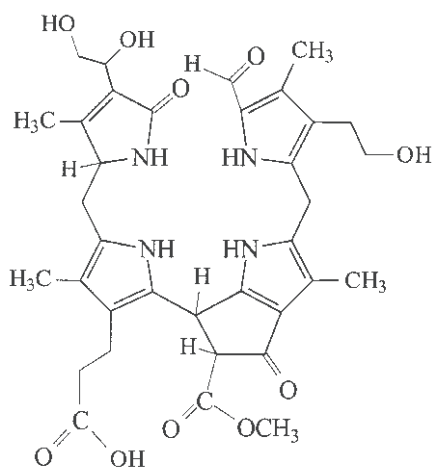

1: *Hv*-NCC-1

Scheme 1

Abbreviations: A. – Arabidopsis; *acd* – accelerated cell death; ALA – aminolevulinic acid; *B. – Brassica*; *C. – Chlorella*; Chl – chlorophyll; Chlide – chlorophyllide; *E. – Escherichia*; *F. – Festuca*; FCC – fluorescent chlorophyll catabolite; LHCP – light harvesting chlorophyll protein; *lls* – lethal leaf spot; MRP – multidrug resistance-associated protein; MS – mass spectrometry; NCC – non-fluorescent chlorophyll catabolite; NMR – nuclear magnetic resonance; PaO – pheophorbide *a* oxygenase; pFCC – primary fluorescent chlorophyll catabolite; Pheide – pheophorbide; RCC – red chlorophyll catabolite

(Matile et al., 1988). Incorporation of ^{14}C isotopic label from [4-^{14}C]-5-aminolevulinic acid (ALA) into these 'rusty pigments' suggested that Chl was their precursor (Peisker et al., 1990). One of these so-called 'rusty pigments', earlier known as RP-14 but now designated as *Hv*-NCC-1 (**1**) (Kräutler et al., 1991), was identified by mass spectrometry (MS) and nuclear magnetic resonance (NMR) spectroscopy as 3^1,3^2,8^2-trihydroxy-1,4,5,10,15,20-(*22H*,*24H*)-octahydro-13^2-[methoxycarbonyl]-4,5-dioxo-4,5-seco-phytoporphyrinate, a colorless catabolite of Chl *a* (**2a**) (see Scheme 1 and section II.C: also Kräutler et al., 1991; 1992); the numbering system used for the linear tetrapyrroles follows that of the Chls (Moss, 1987)). This work on the first structure of a non-green Chl catabolite from plants provided the first clues about Chl catabolism during plant senescence (Matile et al., 1996, 1999; Hörtensteiner, 1999; Kräutler and Matile, 1999; Kräutler, 2003).

II. Chlorophyll Breakdown and Chlorophyll Catabolites in Higher Plants

A. Early Events in Chlorophyll Breakdown

The structure of *Hv*-NCC-1 (**1**) was consistent with dephytylation of Chl *a* (**2a**) as one of the first events of Chl breakdown. In the early 20th century, Arthur Stoll (1912) contributed to this subject by discovering chlorophyllase which catalyses the enzymatic hydrolysis of Chl *a* (**2a**) yielding chlorophyllide (Chlide) *a* (**3a**) and phytol (see Scheme 2). Chlorophyllase thus removes the lipophilic phytol anchor of the Chl molecules, which is necessary for binding the green pigment to the Chl-binding proteins and for insertion of the Chl-protein complexes into the thylakoid membranes of chloroplasts (Paulsen et al., 1993).

Until recently, chlorophyllase was the only known enzyme of the Chl degradative pathway: the subsequent steps remained enigmatic, as further Chl catabolites were unknown. We now know (Bachmann et al., 1994; Matile et al., 1996), that the hydrolytic loss of phytol sets the stage for further enzymatic degradation of both the Chlide and the proteins (Thomas and Hilditch, 1987).

Chlorophyllase is localized in the chloroplast envelope (Matile et al., 1997) and exhibits a remarkable latency. Although it is constitutively present, chlorophyllase activity can only be measured in vivo in the presence of high concentrations of detergents or solvents (Trebitsh et al., 1993); further, the in vivo expression of chlorophyllase in orange fruit requires induction by ethylene and methyl jasmonate

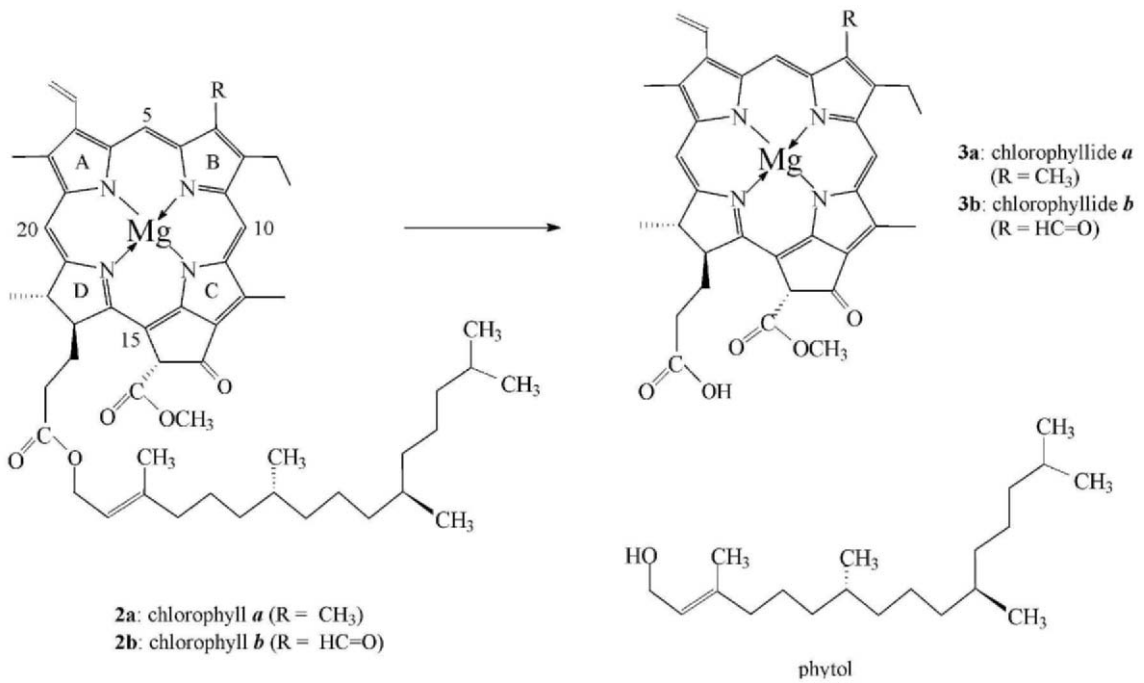

Scheme 2

(Jacob-Wilk et al., 1999). Chlorophyllase has been purified from different plant sources (Trebitsh et al., 1993; Tsuchiya et al., 1997) and has been cloned and functionally over-expressed in *Escherichia* (*E.*) *coli* (Jacob-Wilk et al., 1999; Tsuchiya et al., 1999). The cloned chlorophyllase proteins all contained a highly conserved serine lipase motif, but otherwise the overall homology was rather low (30–40%). Chlorophyllase hydrolyses or transesterifies Chl *a* (**2a**), Chl *b* (**2b**) and the demetallated pheophytin *a* (**4a**), but not the phytyl ester of magnesium protochlorophyllide (**5**) (see Scheme 3) (McFeeters, 1975; Hynninen, 1991).

Remarkably, the Chl catabolites detected in extracts from vascular plants were all derived from Chl *a* (**2a**) and none from Chl *b* (**2b**), the 7-formyl analogue of **2a** (Kräutler and Matile, 1999; Hörtensteiner, 1999; Kräutler, 2003). The fate of Chl *b* (**2b**) during Chl breakdown was, therefore, of particular concern (Matile et al., 1996; Kräutler and Matile, 1999) but the recent discovery of a biochemical pathway from the *b*-type to the *a*-type chlorophyll(ide)s (Chapter 14, Rüdiger) now provides a clue for the absence of Chl *b*-type catabolites (Ito et al., 1993; Ito and Tanaka, 1996; Scheumann et al., 1996; 1999). The well-known oxidative biochemical link between the *a*-type and the *b*-type Chls (Porra et al., 1994; Tanaka et al., 1998) has thus obtained an unexpected reductive counterpart which, together, establish a 'Chl *a*/Chl *b* cycle' (Rüdiger, 1997; Chapter 14, Rüdiger). The reductive step to Chl *a* may function as a very early and obligatory step in Chl *b* breakdown (Ohtsuka et al., 1997; Rüdiger, 1997) in higher plants; indeed, Chl *b* reductase activity is enhanced during senescence (Scheumann et al., 1999). The Chl b reductase and the 'Chl cycle' may also participate in regulating Chl *a/b* ratios in plants during acclimation of the photosynthetic apparatus to changing light intensities (Rüdiger, 1997). These discoveries were consistent with other findings that pheophorbide *a* oxygenase (PaO), the crucial oxygenase which is specifically expressed during senescence, cleaves the chlorin macrocycle of pheophorbide (Pheide) *a* (**6a**), but is inhibited by Pheide *b* (**6b**) (see Section II.B. below) (Hörtensteiner et al., 1995). Thus, the reductive transformation of Chlide *b* (**3b**) to Chlide *a* ensures the availability of all plant Chls for the 'Pheide *a*' degradative pathway (Hörtensteiner, 1999; Matile et al., 1999; Hörtensteiner and Kräutler, 2000). Analysis of the deuterium content of the non-fluorescent Chl

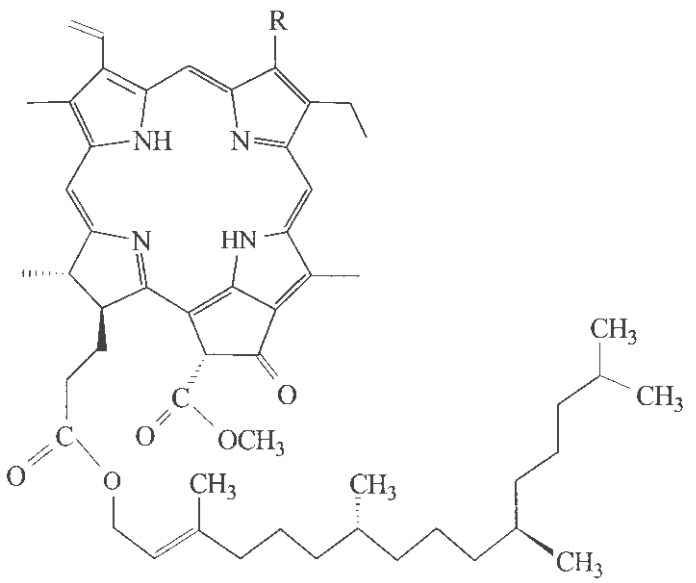

4a: pheophytin ***a*** (R = CH_3)
4b: pheophytin ***b*** (R = HC=O)

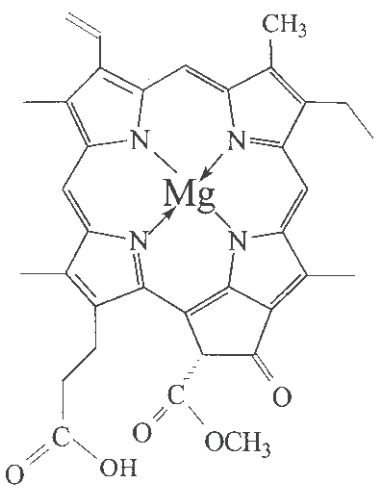

5: Mg-protochlorophyllide

Scheme 3

catabolite *Hv*-NCC-1 (**1**), obtained from artificially degreened primary leaves of barley, provided further independent evidence for the operation of a Chl(ide) *b* (to *a*) reduction in Chl catabolism during senescence (Folly and Engel, 1999).

Most available information suggests that dephytylation and reductive conversion of *b*-Chl(ide)s to *a*-type analogues precedes the loss of the magnesium ion (Langmeier et al., 1993; Shioi et al., 1996a). While the magnesium ion is easily removed from Chlide *a* (**3a**) with dilute acid to generate Pheide *a* (**6a**) (see Scheme 4), a magnesium dechelatase activity has been detected in senescent leaves of *Chenopodium album* (Shioi et al., 1996a) as well as in oilseed rape, *Brassica* (*B.*) *napus* (Langmeier et al., 1993). In the former, it is reported that the magnesium ion is removed and sequestered by a low molecular weight and heat stable 'magnesium dechelating substance' (Shioi et al., 1996a). Much of the magnesium, liberated by Chl degradation during senescence, is transported out of the senescent leaves and stored in the remaining parts of the plant (Matile, 1987).

Pyropheophorbide *a* (**7**), observed in *C. fusca*, *Euglena gracilis* and *Chenopodium album,* has been considered an 'early' Chl catabolite in these green organisms (Schoch et al., 1981; Ziegler et al., 1988; Shioi et al., 1991) and an enzyme, referred to as a 'decarbomethoxylase,' was isolated from *Chenopodium album* (Shioi et al., 1991). Consistent with this, the green alga *Chlamydomonas reinhardtii* showed accumulation of Pheide *a* (**6a**) and of pyropheophorbide *a* (**7**) (Doi et al., 2001) when senescence was artificially induced by lack of light but Chl degradation, beyond the stage of green pigments, was blocked by strictly anaerobic conditions. While these observations suggest enzymatic loss of the 13^2-methoxycarbonyl group in senescing plant leaves and algae during an early phase of Chl breakdown, all presently known colorless, non-fluorescent Chl catabolites from higher plants still possess a methoxycarbonyl function or a carboxylic acid function at C13^2 (Kräutler,` 2003). Indeed, a non-green tetrapyrrolic Chl catabolite having a 13^2-methylene group (as in the pyropheophorbides) has not been isolated from senescent higher plants (Kräutler, 2003; Berghold et al., 2004).

More recent investigations with *Chenopodium album*, however, suggested that only hydrolysis of the methyl ester function of Pheide *a* (**6a**) was enzyme-catalyzed, as significant amounts of 13^2-carboxy-pyropheophorbide *a* (**8**) could be identified by chromatography (Shioi et al., 1996b). The active enzyme, now tentatively named 'pheophorbidase', was specific for chlorins with the highest affinity for Pheide *a* (K_m 12.5 μM). In addition, the reaction was inhibited by methanol, a presumed product of the demethylation (Shioi et al., 1996b). The β-keto-carboxylic acid function of the dicarboxylic acid **8** was found to readily undergo non-enzymatic

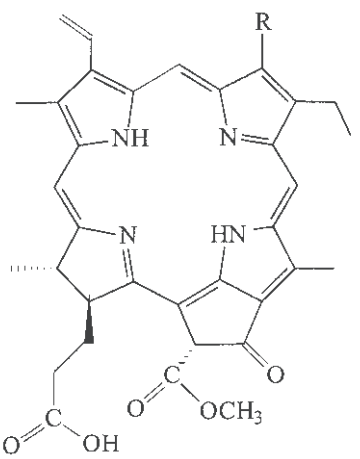

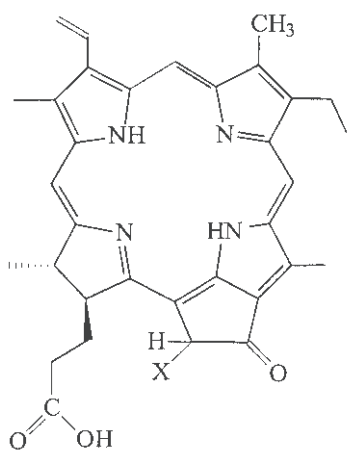

6a: pheophorbide ***a*** (R = CH_3)
6b: pheophorbide ***b*** (R = CH=O)

7: pyropheophorbide ***a*** (X = H)
8:13^2-carboxy-pyropheophorbide ***a*** (X = CO_2H)

Scheme 4

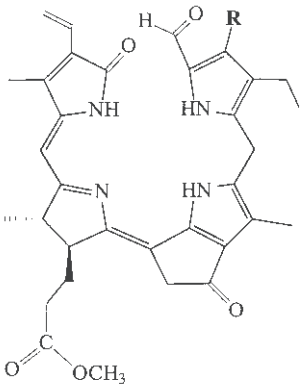

9a: methyl-4,5-dioxo-4,5-seco-pyropheophorbidate *a* (R = CH_3)
9b: methyl-4,5-dioxo-4,5-seco-pyropheophorbidate *b* (R = HC=O)

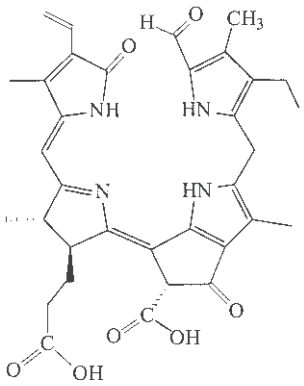

10: 13^2-carboxy-4,5-dioxo-4,5-seco-pyropheophorbide *a*

Scheme 5

decarboxylation at ambient temperature to give the pyropheophorbide *a* (**7**) (Shioi et al., 1996b; Doi et al., 2001). Mühlecker and Kräutler (1996) had suggested the feasibility of the non-enzymatic origin of the latter (see Scheme 4). Likewise, the original characterization of the red, ring-opened derivative (**9a**) of pyropheophorbide from Chl breakdown in the green alga *C. prototheco*ides (Engel et al., 1991) was found more recently to be due to a non-enzymatic decarboxylation during work-up of the corresponding dicarboxylic acid **10** (see section III and Scheme 5; also Engel et al., 1996; Gossauer and Engel, 1996). Currently, therefore, no direct link exists between the observation of pyropheophorbide *a* (**7**) and the later stages of Chl catabolism in higher plants (and green algae).

B. Central Steps of Chlorophyll Breakdown

Colorless, non-fluorescent Chl catabolites have been observed in several senescent vascular plants (Kräutler and Matile, 1999; Kräutler, 2003). When high rates of Chl breakdown were observed in senescent cotyledons of oilseed rape, tiny amounts of nearly colorless but fluorescent compounds were fleetingly observed (Bachmann et al., 1994). These compounds were named 'fluorescent Chl catabolites' (FCCs), because ^{14}C-labeling by [4-^{14}C]-ALA identified them as porphyrin derivatives (Matile et al., 1992; Ginsburg et al., 1994). The FCCs did not accumulate in vivo and were thus deemed to be early, possibly 'primary', products of cleavage of the porphinoid macrocycle of **6a**. This assumption was supported by their location in intact chloroplasts of senescent barley leaves, from which (under appropriate conditions) they were released (Matile et al., 1992).

Another clue about the early steps in Chl breakdown was the discovery that Pheide *a* (**6a**), but not Pheide *b* (**6b**), accumulated in a *F. pratensis* mutant which stays green during senescence (Vicentini et al., 1995a). Also, the accumulation of polar green pigments occurred only in the absence of O_2 (Thomas et al., 1989) suggesting, therefore, that O_2 and **6a** were common substrates in an enzymatic oxidation during Chl breakdown. Similarly, as mentioned above, senescent cells of *Chlamydomonas reinhardtii,* accumulated Pheide *a* (**6a**) or pyropheophorbide *a* (**7**) in the absence of O_2 (Doi et al., 2001).

1. Enzymatic Experiments with Synthetically-derived Red Chlorophyll Catabolite

Determination of the structure of the 'primary' fluorescent Chl catabolite (pFCC; **11**) as (3^1,3^2-didehydro-1,4,5,10,17,18,20,(*22H*)-octahydro-13^2-(methoxycarbonyl)-4,5-dioxo-4,5-seco-phytoporphyrin, see Scheme 6) (Mühlecker et al., 1997) suggested that the key step in Chl breakdown was an oxygenolytic

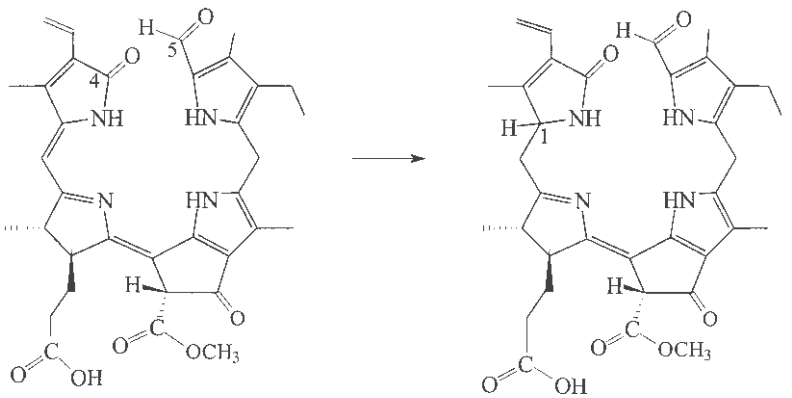

12: "red" chlorophyll catabolite (RCC)

11: "primary" fluorescent chlorophyll catabolite (pFCC)

11-*epi*: 1-*epi*-pFCC (C(1)-epimer of pFCC)

Scheme 6

cleavage at the 'northern' C5 position of the porphinoid macrocycle of Pheide *a* (**6a**) by an elusive oxygenase (Ginsburg and Matile, 1993; Hörtensteiner et al., 1995), followed by hydrogenation of the 'western' C20 meso position, thus generating the pFCC (**11**). Consequently, the 'red chlorophyll catabolite' (RCC) **12** (3^1,3^2-didehydro-4,5,10,17,18,(*22H*)-hexahydro-13^2-(methoxycarbonyl)-4,5-dioxo-4,5-seco-phytoporphyrin) was proposed as a precursor of pFCC (**11**), since it differed only by addition of two hydrogen atoms at C1 and C20. This suggested that RCC (**12**), which shared the same chromophore structure as some red bilinones excreted as final Chl degradation products by *C. protothecoides* (Engel et al., 1996; Gossauer and Engel, 1996), was an intermediate in Chl breakdown in higher plants (Mühlecker et al., 1997).

By analogy to the earlier chemical preparation of red tetrapyrrolic isolate **9a** from *C. protothecoides* by Iturraspe and Gossauer (1992), RCC **12** could be prepared in a sequence of five chemical steps by partial degradation of methyl pheophorbidate *a* (**13**) via methyl-4,5-dioxo-4,5-seco-pheophorbidate **14** (RCC methyl ester; see Scheme 7; also Kräutler et al., 1997; and reviewed in Kräutler, 2003). The UV/Vis-spectrum of the weakly fluorescing red diester **14** has prominent absorbance maxima near 500 and 316 nm (Fig. 1). The diester **14** was spectroscopically identical with the methylation product of the di-acid **10** from the green alga *C. protothecoides* (Gossauer and Engel, 1996; Kräutler et al., 1997).

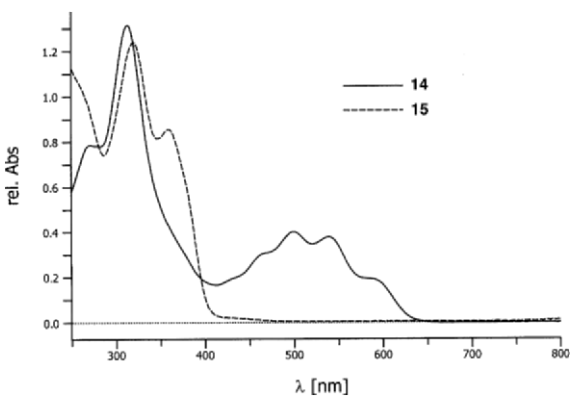

Fig. 1. UV/Vis-spectra of RCC methyl ester (**14**, in chloroform) (Kräutler et al., 1997) and of the methyl ester of pFCC (**15**, in methanol) (Oberhuber and Kräutler, 2002).

With the authentic RCC (**12**) now available (Kräutler et al., 1997), the identical red compound was found in senescent plants as the elusive RCC in the experiments of Rodoni et al. (1997a,b): small amounts of the red compound **12** were obtained from Pheide *a* (**6a**) by enzyme-catalyzed oxygenolysis during aerobic incubation with extracts of washed senescent canola chloroplast membranes supplied with reduced ferredoxin. The identity of the elusive RCC, thus produced, was confirmed by co-chromatography with synthetic **12** using HPLC. The enzymatic activity in the washed senescent chloroplast membranes was achieved by a single enzyme, an oxygenase meanwhile termed PaO. The putative oxygenase possessed a non-heme

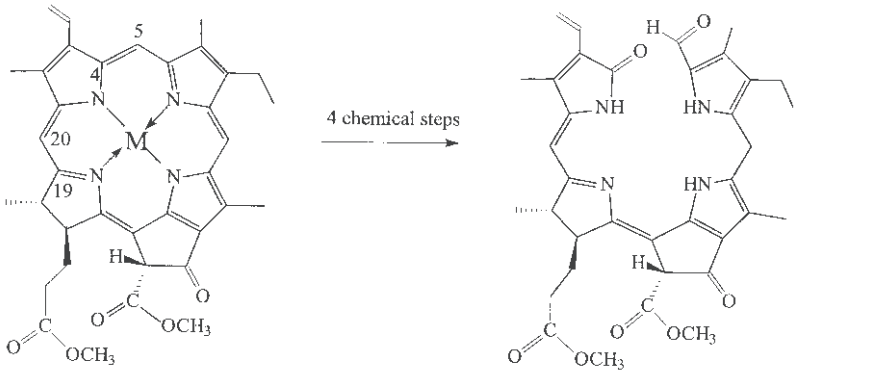

13: methyl-pheophorbidate *a* (M = 2H)

14: methyl-4,5-dioxo-4,5-seco-pheophorbidate *a* (RCC methyl ester)

Scheme 7

iron-containing reactive center as shown by the in vitro and *in organello* inhibition of fluorescent catabolite formation by chelators, such as 2,2′-dipyridyl (Schellenberg et al., 1990; Hörtensteiner et al., 1995). Thus, the enzyme was probably related to other non-heme iron-dependent (mono)oxygenases (Lippard and Berg, 1994).

Anaerobic incubation of chemically-prepared RCC (**12**) with stroma proteins, isolated from barley chloroplasts, and reduced ferredoxin produced three fluorescing compounds which had the same UV/Vis-spectrum as the pFCC **11**: one of these compounds shared identical HPLC characteristics with pFCC (**11**) (Rodoni et al., 1997a,b).

2. Pheophorbide a Oxygenase Cleaves the Porphyrin Macrocycle

PaO catalyzes the crucial and (effectively) irreversible cleavage of the porphinoid macrocycle and may be considered to represent a key enzyme of Chl breakdown. Since the oxygenolytic transformation of Pheide *a* to enzyme-bound **12** involves O_2 (Rodoni et al., 1997a), this transformation could be achieved either by a mono-oxygenase or by the joint action of a dioxygenase and a reductase. An in vitro assay of PaO was developed using an oilseed-rape preparation containing partially purified oxygenase and the reductase (see below; see also Hörtensteiner et al., 1998). As the oxygenase was known to be inhibited by its product (Hörtensteiner et al., 1995), the presence of the reductase was essential to achieve useful turn-over and the reduction product, pFCC (**11**), was analyzed. In the presence of $^{18}O_2$, this active enzyme mixture converted Pheide *a* (**6a**) into ^{18}O-labeled pFCC (**11**-^{18}O) containing one ^{18}O-atom per molecule of catabolite, as determined by MS analysis of the molecular ion (see Scheme 8). From MS analysis of fragmentation ions of **11**-^{18}O, the isotopic label was localized to the formyl group attached to 'ring B' thus indicating the incorporation of one oxygen atom from O_2 at the C5 position of **6a**. As only one of the two oxygen atoms introduced in the oxidation of **6a** to **12** is derived from O_2, PaO is a mono-oxygenase and the other oxygen atom is, most likely, derived (directly or indirectly) from water (Hörtensteiner et al., 1998).

As attempts to purify PaO were not overly successful (Hörtensteiner et al., 1998) a functional genomic approach was used to clone PaO. Exploiting known biochemical properties of PaO, the *A. thaliana* protein database (Arabidopsis Genome Initiative, 2000) was screened for candidate proteins that may encode PaO. From 21 proteins identified this way, one protein (At3g44880) was subsequently shown to encode *A. thaliana* PaO (AtPaO) (Pružinská et al., 2003). Thus, the biochemical properties of the recombinant protein were identical to PaO isolated from natural sources. AtPaO is a Rieske-type iron-sulfur protein that is identical to the previously identified *A. thaliana* accelerated cell death 1 (ACD1) and homologous to lethal leaf spot 1 (LLS1) from maize (Gray et al., 2002). Using a *lls1* mutant, the function of PaO could be confirmed: *lls1* leaves showed a stay-green phenotype in the dark and accumulated Pheide *a* upon senescence induction (Pružinská et al., 2003).

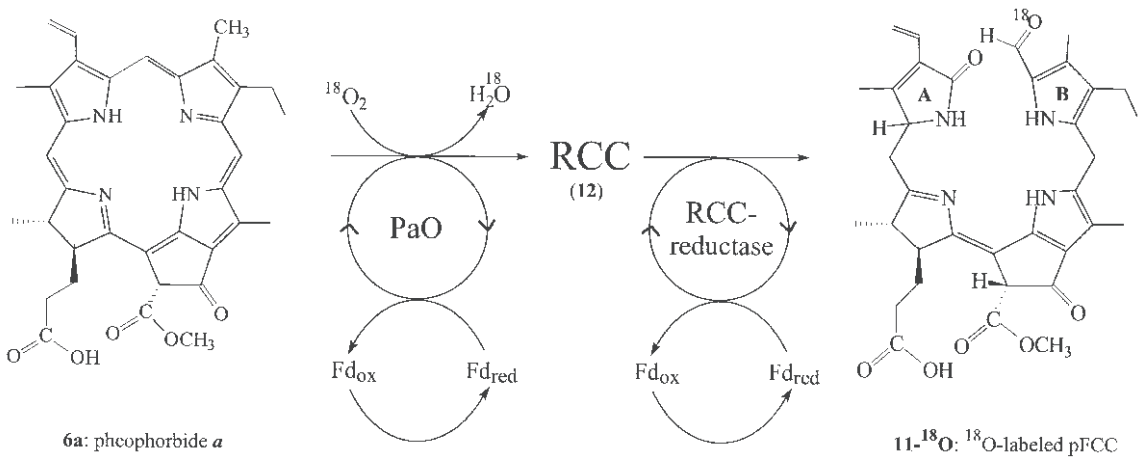

6a: phcophorbide *a*

11-^{18}O: ^{18}O-labeled pFCC

Scheme 8

The enzymatic oxidation of Pheide *a* (**6a**) into the RCC, **12,** by PaO is a remarkable structural transformation. The oxygenase is intriguingly specific for Pheide *a* (**6a**) (Hörtensteiner et al. 1995), and ferredoxin drives its redox cycle (Schellenberg et al., 1993). Besides the incorporation of two oxygen atoms, the ring opening at the newly oxygenated sites includes also formation of two carbonyl functions and the saturation of the 'eastern' C10 meso position. Formally, **12** arises from Pheide *a* (**6a**) by addition of one equivalent each of dioxygen and dihydrogen, but the mechanism of the hypothetical isomerization of the primary enzymatic oxygenation product to the ring-opened (enzyme-bound) form of **12** is not clear. Section III describes the related problem of the formation of red catabolites (such as **9a** and **10**) in the green alga *C. protothecoides* (Curty et al., 1995; Gossauer and Engel, 1996; Curty and Engel, 1997).

Chl breakdown and the process catalyzed by PaO had a crucial impact on the development of the laws of genetics that Mendel established in the 19th century (Mendel, 1865). The puzzling observation of the phenotype of a recessive allele in Mendel's 'green peas' is now known to be connected to a deficiency of the activity of this oxygenase (Thomas et al., 1996). In addition, a stay-green mutant of *F. pratensis*, Bf 993, which is unable to degreen during senescence, has been demonstrated to be biochemically deficient in PaO (Vicentini et al., 1995a). The mutation of Bf 993 is inherited as a single recessive gene, *sid* (Thomas, 1987) suggesting that the *Sid* locus encodes or regulates the gene for PaO.

3. Red Chlorophyll Catabolite Reductase Produces Colorless, Fluorescent Chlorophyll Catabolites

As described above, RCC (**12**) is bound strongly to the membrane-attached oxygenase, PaO, and inhibits further oxygenase activity; however, a stromal reductase, employed in an in vitro assay (see above), reduces authentic **12** to pFCC (**11**) which is no longer enzyme bound (Mühlecker et al., 1997; Rodoni et al., 1997a). This reductase, named RCC reductase (Rodoni et al., 1997a; Wüthrich et al., 2000), is dependent on reduced ferredoxin as electron donor (Wüthrich et al., 2000). As the cleavage of the Chl macrocycle in higher plants requires the intimate cooperation of the membrane-bound PaO and the stromal RCC reductase, it may represent an example of 'metabolic channeling' (Rodoni et al., 1997a,b; Matile et al., 1999). Evidence for this is the lack of accumulation of RCC in coupled in vitro assays of PaO activity. RCC reductase produces pFCC by stereospecifically reducing C1 of PaO-produced (and enzyme-bound) **12**. However, authentic chemically-derived **12** was transformed to three FCCs by tissue extracts containing RCC-reductase (Rodoni et al., 1997a; Wüthrich et al., 2000), suggesting that the interaction with PaO confers stereospecificity to RCC reductase (Wüthrich et al., 2000). Further, the finding that RCC reductase activity is inhibited by O_2 (Rodoni et al., 1997a,b), while PaO requires O_2 for activity (Hörtensteiner et al., 1998), supports the idea of a PaO-RCC reductase interaction, whereby O_2 consumption by PaO could

generate an O_2-depleted micro-environment at the site of RCC-reductase activity.

The molecular formula of **11** ($C_{35}H_{40}N_4O_7$) determined from high-resolution MS, indicated **11** to be derived from **6a** by formal addition of one equivalent of O_2 and two equivalents of H_2. By NMR spectroscopy, **11** was identified as $3^1,3^2$-didehydro-1,4,5,10,17,18,20(*22H*)-octahydro-13^2(methoxycarbonyl)-4,5-dioxo-4,5-seco-phytoporphyrin, a linear tetrapyrrole derived from Pheide *a* by an oxygenolytic cleavage at the 'northern' C5 meso position and by reductive saturation of the 'western' C20 and C1 positions (Mühlecker et al., 1997). This structure clearly showed **11** to be an intermediate in Chl catabolism preceding the stage of the 'non-fluorescent' Chl catabolites (NCCs, see below). Meanwhile, a second fluorescent Chl catabolite (**1**-*epi*-pFCC, **11**-*epi*) was isolated from sweet pepper (*Capsicum annuum*) and its structure was determined (Mühlecker et al., 2000): **11**-*epi* was shown to be a stereoisomer of **11** differing only in its configuration at C1, the asymmetric carbon center newly-introduced by the two highly stereo-selective RCC reductases present in sweet pepper and oilseed rape (Hörtensteiner et al., 2000; Mühlecker et al., 2000). Thus, these two FCCs (**11** and **11**-*epi*) are direct reduction products of two different RCC reductases and both should, therefore, be considered as pFCCs (Mühlecker et al., 1997, 2000). The UV/Vis-spectrum of 11 and of 11-*epi* shows two prominent absorption bands, near 361 and 320 nm (see Fig. 1), and solutions of the pFCCs possess a luminescence maximum near 436 nm. The remarkable stereo-dichotomy of the respective RCC reductases of the two plant species indicates an apparent functional irrelevance of the absolute configuration at the C1 chiral center generated by these reductases (Mühlecker et al., 2000). Meanwhile, screening a variety of plant species by HPLC for their pFCC epimer type revealed a species-dependent distribution of the two classes of RCC reductases (Hörtensteiner et al., 2000): within a plant family, all genera and species produce the same epimeric pFCC. The RCC reductase activity found in the ancient terrestrial species, *Selaginella* (Hörtensteiner et al., 2000) and the livermoss *Marchantia polymorpha* (Wüthrich et al., 2000), but not in the green alga *C. prototheco*ides (S. Hörtensteiner, unpublished), indicates that the 'invention' of RCC reductase might have been an important evolutionary step from the unicellular aquatic stage to multicellular land plants; indeed, in *C. prototheco*ides, Chl catabolism ends with the excretion of RCC-like linear tetrapyrroles into the medium (Section III).

RCC reductase has been purified from senescent barley primary leaves (Rodoni et al., 1997b; Wüthrich et al., 2000) and a cDNA fragment was subsequently isolated. Database searches identified homologous sequences from different species, and RCC-reductase from *A. thaliana* (AtRCCR) was cloned and functionally expressed in *E. coli* (Wüthrich et al., 2000). Recombinant AtRCCR converted chemically-prepared RCC (**12**) (Kräutler et al., 1997) to the epimeric pFCCs, **11** and **11**-*epi*. As observed with native RCC reductase (Hörtensteiner et al., 2000), when heterologously-expressed AtRCCR was assayed in the presence of PaO (Wüthrich et al., 2000), the reaction was stereo-selective for the production of **11**. In barley and *A. thaliana*, RCC reductase is encoded by a single copy gene which seems to be constitutively expressed. Independently, an *accelerated cell death 2* (*acd2*) mutant of *A. thaliana* was identified (Greenberg et al., 1994) which is defective in the RCC reductase gene (Mach et al., 2001). This mutant spontaneously forms spreading lesions and activates a constitutive pathogen defense even in the absence of pathogen infection. This hypersensitive reaction only occurred in the light, suggesting that the Chl catabolic pathway has an important role in disease resistance by removing photoactive Chl catabolites.

That RCC reductase required no cofactors, other than reduced ferredoxin, for reduction of RCC (**12**) to form **11** appeared puzzling and suggested that the enzyme-bound RCC (**12**) was a sufficiently redox-active substrate to undergo a ferredoxin-driven reduction to form 11 without requiring further reducing cofactors. To test this assumption, the electrochemical reduction of the methyl ester (**14**) of RCC, available from partial synthesis (Kräutler et al., 1997), was studied in both analytical and preparative electrochemical experiments (Oberhuber and Kräutler, 2002); indeed, electrochemical reduction of **14** in methanol at room temperature proceeded stereo-unselectively and gave two major compounds with UV/Vis-absorbance properties of pFCC, **11** (see Fig. 1). It resulted in about 12% each of the strongly luminescent tetrapyrroles, **15** and **15**-*epi*, the methyl esters of the two epimeric pFCCs, **11** and **11**-*epi*, (see Scheme 9). In addition, about 30% of a new type of reduction products was formed which possessed a different chromophore structure with a UV/Vis-spectrum showing peaks near 310 and 420 nm. MS studies showed the four main

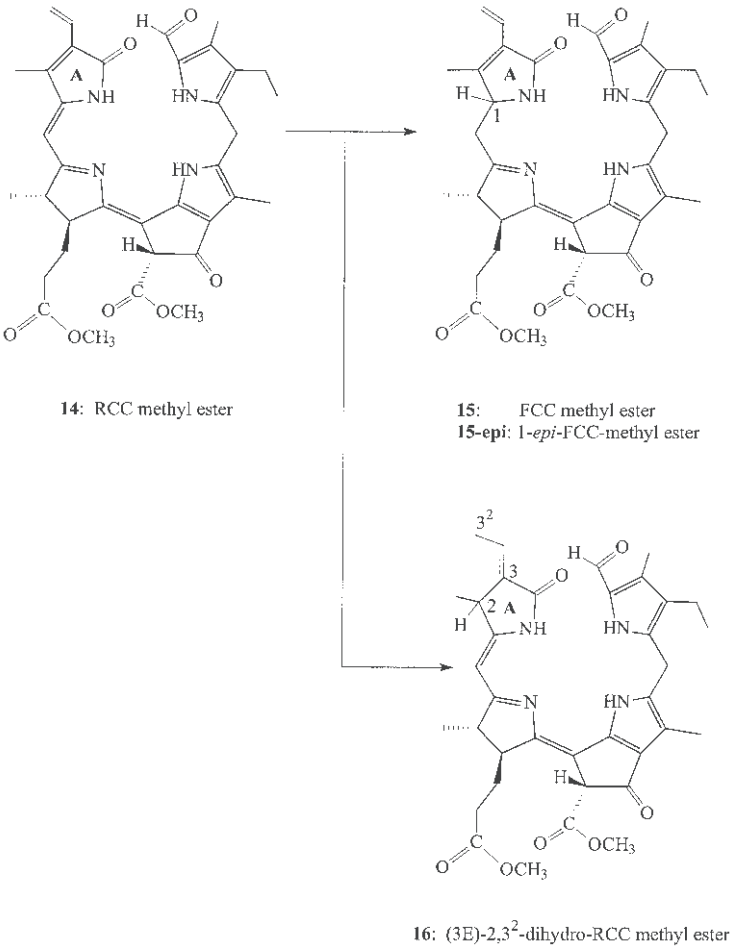

Scheme 9

fractions to have the same molecular formula as **15**. The almost non-fluorescent linear tetrapyrrole **16** and its three stereoisomers were further characterized by NMR-spectroscopy (Oberhuber and Kräutler, 2002). They were found to differ in their stereochemistry at C2- and C13^2 and to be linear tetrapyrrolic reduction products with an ethylidene group on ring A; that is, to be regio-isomers of **15**. The structures of the methyl-3^1,3^2-didehydro-1,4,5,10,17,18,20*(22H)*-octahydro-13^2-(methoxycarbonyl)-4,5-dioxo-4,5-seco-(22H)-phyto-porphyrin (**15**) and of the methyl-3^1-dehydro-2,4,5,10,17,18,22-heptahydro-13^2-(methoxycarbonyl)-4,5-dioxo-4,5-seco-(22H)-phytoporphyrin (**16**), as well as of their stereo-isomers, were spectroscopically determined. These two electrochemical reduction paths to **15** and **16** are reminiscent of the known pair of isomeric enzymatic reductions of biliverdin (**17**) to phytochromobilin (**18**) and 15,16-dihydrobiliverdin (**19**) (Beale and Weinstein, 1991; Beale and Cornejo, 1991).

These electrochemical model experiments suggest, therefore, that RCC (**12**) is sufficiently redox-active to undergo ferredoxin-driven and enzyme mediated reduction to **11** or **11**-*epi* (Oberhuber and Kräutler, 2002); thus, reduction of RCC by RCC reductase may occur in single electron reduction and protonation steps. The following functions can therefore be assigned to RCC reductase:

(i) binding PaO with bound **12** and reduced ferredoxin,

(ii) mediating the electron transfer reactions from ferredoxin to the bound substrate, and

(iii) controlling properly the regio- and stereo-selective protonation at C20 and C1 of the protein-bound tetrapyrrolic reduction intermediates.

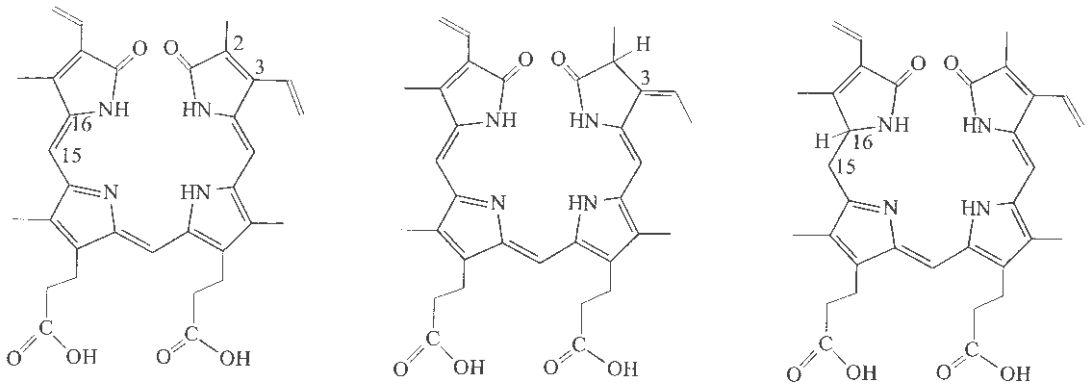

17: biliverdin **18**: (3Z)-phytochromobilin **19**: 15,16-dihydrobiliverdin

Scheme 10

In this model, RCC reductase would not carry out the reduction steps, but would direct them in an optimal way in the manner of a 'chaperone.'

RCC reductases show remarkable homology with some ferredoxin-dependent biliverdin reductases (Frankenberg et al., 2001). Not only the sequence homologies but also the requirement for ferredoxin as a reductant (Wüthrich et al., 2000), as well as the similar chemical transformations catalyzed by these reductases indicate unexpected similarities between the biodegradation of heme (Beale and Cornejo, 1991; Falk, 1989) and Chl in higher plants (Hörtensteiner et al., 2000; Oberhuber and Kräutler, 2002).

C. Late Stages of Chlorophyll Breakdown

The chemically labile, fluorescent Chl catabolites, such as pFCC (**11**), do not accumulate during Chl breakdown in vascular plants, but are readily transformed further to the colorless NCCs, such as *Hv*-NCC-1, (**1**, 3^1,3^2,8^2-trihydroxy-1,4,5,10,15,20-(*22H*,*24H*)-octahydro-13^2-(methoxycarbonyl)-4,5-dioxo-4,5-seco-phyto-porphyrinate, (see Fig. 1 for structure of **1** and Fig. 2 for UV- and CD-spectra; also Kräutler et al., 1991, 1992; Kräutler, 2003). The colorless NCCs are the first linear tetrapyrrolic intermediates during chlorophyll breakdown, in which the four pyrrolic units are completely de-conjugated. A direct isomerization of FCCs to the corresponding NCCs may achieve this result (Mühlecker et al., 1997; Kräutler and Matile, 1999; Hörtensteiner and Kräutler, 2000). Such a reaction is likely to be thermodynamically favorable, by analogy with studies of the tautomerization of various hydro-porphinoids (Eschenmoser, 1988). Indeed, recent non-enzymatic experiments showed the stereo-selective isomerization of the authentic *p*FCC **11**-*epi* to the NCC **21** (see Scheme 11) to occur very readily at ambient temperatures and in weakly acidic aqueous medium (Oberhuber et al., 2003). Therefore, this 'final stage' in the natural breakdown of the intensely-colored Chl into colorless NCCs possibly occurs under rather mild, non-enzymatic, conditions.

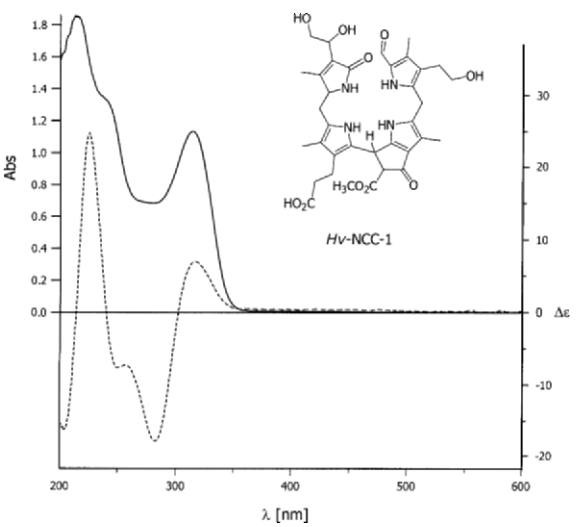

Fig. 2. UV-/Vis- (—) and CD-spectra (- - -) of the nonfluorescent chlorophyll catabolite *Hv*-NCC-1 (**1**, in water) (Kräutler et al., 1992).

Careful re-analysis of extracts of senescent leaves of the tree, *Cercidiphyllum japonicum,* confirmed not only the dominant presence of the non-fluorescent Chl catabolite (*Cj*-NCC-1, **20**) (Curty and Engel, 1996), but also revealed the less polar *Cj*-NCC-2. NMR-spectroscopic analysis showed *Cj*-NCC-2 to be a $3^1,3^2$-didehydro-1,4,5,10,15,20-(*22H,24H*)-octahydro-13^2-(methoxycarbonyl)-4,5-dioxo-4,5-seco-phytoporphyrinate and to be identical with *Cj*-NCC-2, **21**. the latter is is an isomer of a 'primary' FCC (**11** or **11**-*epi*) and is the first of the known NCCs lacking the characteristic hydroxyl function at ring B (see Scheme 11; also Kräutler, 2002; Oberhuber et al., 2003). *Cj*-NCC-2 (**21**) is thus suggested to be formed directly by (nonenzymatic) isomerization of pFCC **11**-*epi* and to be a 'primary' NCC (pNCC) of *Cercidiphyllum japonicum* (Kräutler and Matile, 1999; Hörtensteiner and Kräutler, 2000; Oberhuber et al., 2003).

The timing and the organellar location within the senescent leaf cell (see Fig. 3) of the isomerization of FCCs into the corresponding NCCs during Chl breakdown, have been a matter of special interest (Matile et al., 1996; Hörtensteiner, 1999; Kräutler and Matile, 1999). This (hypothetical) isomerization may occur before, in parallel with or after the side chain modification (refunctionalization) reactions, which are indicated by the structures of the known NCCs (see below). As low pH values are typical of vacuoles, the isomerization of FCCs to NCCs is now suggested to occur as a non-enzymatic process in the vacuoles during the natural course of Chl breakdown. The vacuoles thus appear to be the sites for this final isomerization, as well as the final storage compartment for the NCCs.

As a prerequisite for the isomerization of FCCs to NCCs, the controlled transport of the FCCs to the vacuoles becomes an important event in Chl breakdown. Consideration of the observed side chain functions of the NCCs suggests the availability of polar peripheral groups to be relevant for a carrier-mediated transport (of the FCCs) into the vacuoles. This further suggests that side chain modifications would occur at the level of the pFCCs and in the senescent chloroplasts (Kräutler and Matile, 1999; Hörtensteiner and Kräutler, 2000). Treatment of the pFCC **11** by an active extract of soluble enzymes from degreened cotyledons of oilseed rape produced an FCC with significantly higher polarity which was tentatively assigned the structure of the $3^1,3^2$-didehydro-1,4,5,10,17,18,20-(22H)-octahydro-13^2-(carboxy)-4,5-dioxo-4,5-seco-phytoporphyrin (**22**) (see Scheme 11; Hörtensteiner and Kräutler, 2000). The same extract from senescent cotyledons of oilseed rape did not hydrolyze the methyl ester function in several NCCs, indicating that hydrolysis of the 13^2-methoxycarbonyl function in these senescent leaves occurs at the stage of the FCCs (Hörtensteiner, unpublished). This view is consistent with the observation in senescent leaf extracts of small amounts of unknown

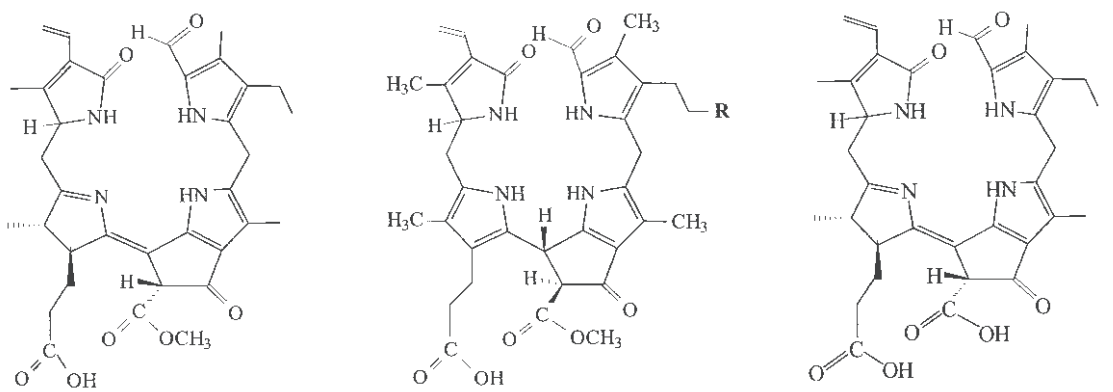

Scheme 11

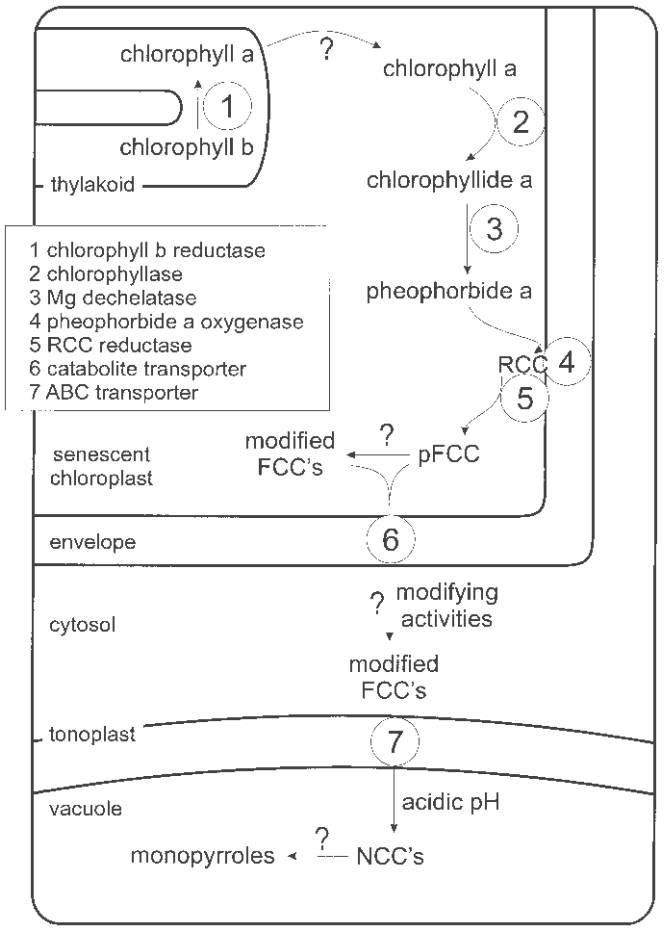

Fig. 3. Topographical overview of the biochemistry of chlorophyll catabolism in higher plants. Numbers refer to enzymes or transporters that are thought to be involved. Putative (enzymatic) steps are indicated with a question mark.

compounds displaying fluorescence properties similar to those of the pFCCs (Hörtensteiner, 1999; Hörtensteiner and Kräutler, 2000).

The discovery in naturally degreened cotyledons of the dicot, *B. napus,* of three NCCs, namely, *Bn*-NCC-1 (**23**), *Bn*-NCC-2 (**24**) and *Bn*-NCC-3 (**25**), which have the same basic structure as **1** (see Scheme 12; Mühlecker and Kräutler, 1996), strengthened the general significance of the original structure of *Hv*-NCC-1 (**1**) as a natural Chl breakdown in higher plants (Ginsburg and Matile, 1993; Mühlecker et al., 1993). Most notably, the *Bn*-NCCs proved to be linear tetrapyrroles which were again derived from Chl *a* (**2a**) by an oxygenolytic ring opening at the 'northern' C5 meso position, while differing from catabolite **1** of barley merely by some of the peripheral side chains (see Scheme 12). More recently, compounds with spectral characteristics of NCCs were also found in autumn leaves of sweet gum, *Liquidambar styraciflua* (Iturraspe et al., 1995), and of *Cercidiphyllum japonicum* (the *Cj*-NCCs, see Curty and Engel, 1996), in naturally degreened leaves of spinach (the *So*-NCCs, see Oberhuber et al., 2001; Berghold et al., 2002) and of tobacco leaves (the *Nr*-NCCs, see Berghold et al., 2004). All NCCs isolated so far from a variety of degreened plants represent linear tetrapyrroles of uniform basic structure (see Schemes 1 and 12) and relate to Chl *a* (**2a**) rather than to Chl *b* (**2b**) (Kräutler and Matile, 1999; Kräutler, 2003). It is noteworthy that *So*-NCC-2 (**26**), the most abundant of the four NCCs detected in spinach, has the same constitution as the catabolite from barley, *Hv*-NCC-1 (**1**), but differs from **1** by the configuration at C1 (**26** and **1** are epimers). With osmium tetroxide, the catabolite *Cj*-NCC-1 (**20**) from *Cercidiphyllum japonicum* (or its methyl ester **27**) could be regio-selectively dihydroxylated at its

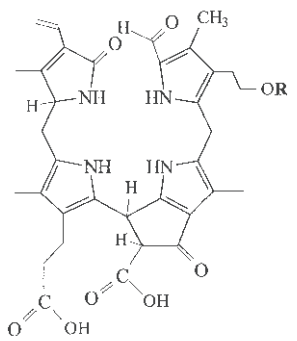

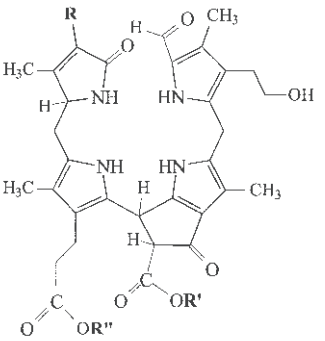

23: *Bn*-NCC-1 R = 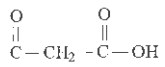

24: *Bn*-NCC-2 R = 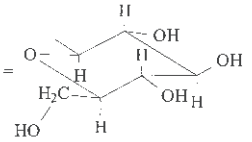

25: *Bn*-NCC-3 R = H

26: *So*-NCC-2 (R = $CH(OH)–CH_2–OH$; R' = CH_3, R" = H)

28: *So*-NCC-3 (R = $CH=CH_2$; R' = R" = H)

29: *So*-NCC-4 (R = $CH=CH_2$; R' = CH_3, R" = H)

27: *Cj*-NCC-1 methyl ester (R = $CH=CH_2$, R' = R" = CH_3)

Scheme 12

vinyl group and one of the two stereo-unselectively prepared dihydroxylation products of **20** proved to be identical with *So*-NCC-2 (**26**) (see Scheme 12; also Oberhuber et al., 2001).

The most remarkable of the peripheral side chain modifications found in the NCCs is the hydroxylation of the terminal position of the ethyl group on ring B which would be difficult to achieve in a non-enzymatic reaction (Kräutler et al., 1991; Kräutler, 2003). The primary alcohol function appears to represent an anchor point for further conjugations with hydrophilic moieties, such as the malonyl group in *Bn*-NCC-1 (**23**) and the β-glucopyranosyl group in *Bn*-NCC-2 (24) (see Scheme 12; also Mühlecker and Kräutler, 1996). Several NCCs with a free 8^2-hydroxyl function could be esterified with a malonyl moiety using a protein preparation from canola cotyledons and malonyl-CoA as co-substrate, while 1-aminocyclopropane-1-carboxylic acid (ACC), the substrate for ACC malonyltransferase, was not accepted as a substrate (Hörtensteiner, 1998). The two tobacco *Nr*-NCCs are also conjugated to glucosyl moieties (Berghold et al., 2004). Esterification and glucosylation, as in **23** and in **24**, are reminiscent of many secondary plant metabolites which are deposited in the vacuoles (Hinder et al., 1996; Matile, 1997).

While all *Bn*-NCCs possess a β-keto carboxylic acid group at $C13^2$ of the characteristic cylopentanone moiety (Hörtensteiner and Kräutler, 2000), the 13^2-methyl ester function of the Chls is retained in *Hv*-NCC-1 (**1**) and in many other NCCs (Kräutler, 2003). Interestingly, in naturally degreened leaves of spinach, *So*-NCC-2 (**26**) and *So*-NCC-3 (**28**) retain the $C13^2$ methyl ester but *So*-NCC-4 (**29**) carries a free β-keto carboxylic acid group at $C13^2$. The occurrence of both the methyl ester and of free acid groups at $C13^2$ in some So-NCCs raises the question of the possible timing of the methyl ester hydrolysis (Berghold et al., 2002).

Currently, the further endogenous breakdown of Chl in senescent plant tissue, beyond the stage of the NCCs, has not been well established and may not follow a specific pathway. Indeed, the NCCs are accumulated in the vacuoles of senescent leaves of higher plants (Hinder et al., 1996; Matile, 1997) and, in samples of degreened cotyledons from oilseed rape, the amount of *Bn*-NCCs present corresponded to the calculated amount of Chls *a* and *b* initially present in the green leaf (Mühlecker and Kräutler, 1996). Further, the total content of NCCs in degreened leaves of barley, oilseed rape and French beans did not markedly decrease over a period of several days (Bortlik et al., 1990; Matile, 1992; Ginsburg and Matile, 1993); thus, the NCCs may be the final products of controlled Chl breakdown in senescent vascular plants (Kräutler and Matile, 1999; Hörtensteiner and Kräutler, 2000).

First evidence of tetrapyrrolic products of further

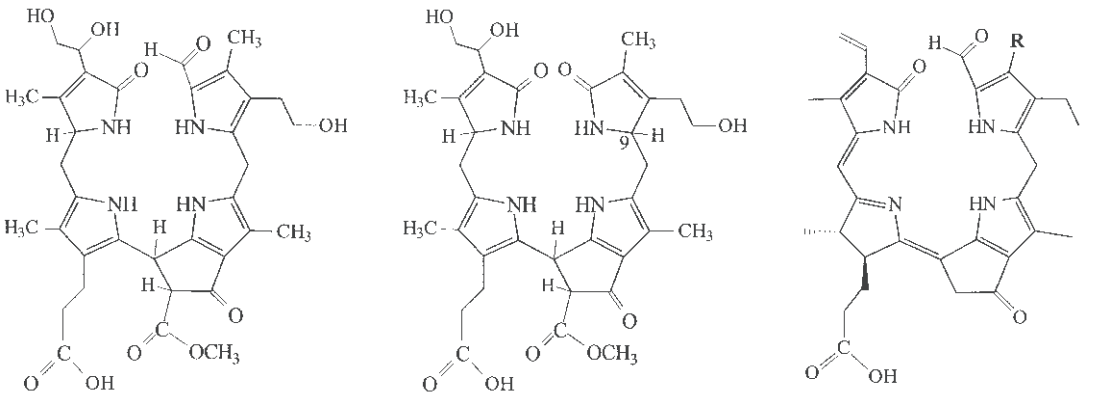

1: *Hv*-NCC-1

30
30-*epi*: C(9)-epimer of **30**

31a: R = CH_3
31b: R = CH=O

Scheme 13

degradation of NCCs was the recent identification of colorless urobilinogen-like linear tetrapyrroles in extracts of degreened primary leaves of barley, described as the two stereoisomers **30** and **30**-*epi* (see Scheme 13). Since both **30** and **30**-*epi* were associated with further degradation of *Hv*-NCC-1 (**1**) by loss of the C5-derived formyl group on ring B, it was suggested they represent a new type of Chl catabolite in barley (Losey and Engel, 2001).

Possibly **30** and **30**-*epi* arise in senescent barley leaves by non-enzymatic oxidative loss of the C5 formyl group of the NCCs as has been noted in related linear tetrapyrroles (Losey and Engel, 2001). Indeed, the original characterization of *Hv*-NCC-1 (**1**) as a 'rusty' pigment indicates the readiness of these colorless reduced linear tetrapyrroles to undergo spontaneous reactions to develop the rust color (Bortlik et al., 1990; Kräutler and Matile, 1999). Clearly, such transformations, as well as the suggested oxidative loss of the formyl group of *Hv*-NCC-1 (**1**), and any further reactions of the NCCs, may be dependent on factors modifying the environment within the senescent plant tissue; for example, further degradation of NCCs in degreened leaves or other plant tissues will depend on their eventual fate, including their further use or their consumption by heterotrophic organisms. Fungal pathogens are also known to exploit and, in some instances, to exert local control over senescence processes in the plants (Hammond-Kosack and Jones, 2001). Earlier considerations of further degradation to monopyrrolic oxygenation products (Llewellyn et al., 1990; Brown et al., 1991) received renewed support from Suzuki and Shioi (1999) who detected hematinic acid, ethyl-methyl-maleimide and a putative degradation product of the C-E-ring moiety of Pheide *a*.

D. Subcellular Organization and Regulation of Chlorophyll Breakdown in Higher Plants

The NCCs, formed during rape- and barley-leaf senescence, accumulate in the central vacuoles of mesophyll cells (Matile et al., 1988; Hinder et al., 1996), whereas Chl resides in the thylakoid membranes of the chloroplast. The different subcellular location of the enzymes of Chl catabolism and the requirement for catabolites to cross intra-cellular membranes raises interesting questions about the subcellular organization of the pathway.

The 'early' Chl breakdown reactions to FCCs occur within the plastids as demonstrated in barley and oilseed rape (Schellenberg et al., 1990; Ginsburg et al., 1994) (see Fig. 3). Chl *b* reductase, which reduces Chl *b* to Chl *a,* is located in the thylakoid membrane (Scheumann et al., 1999).

The second catabolic enzyme, chlorophyllase (see Fig. 3), is located in the plastid membrane system and, in *Citrus* and barley (Brandis et al., 1996; Matile et al., 1997), it was demonstrated on the inner envelope membrane; however, the cloning of chlorophyllases from different plants raises doubts about its plastid membrane location, since no potential trans-membrane domains are present in the amino acid sequences. Further, different subcel-

lular locations were predicted for chlorophyllase by Jacob-Wilk et al. (1999) and Tsuchiya et al. (1999). These latter findings were interpreted in terms of an alternative degradation pathway located outside the plastid (Takamiya et al., 2000). Although chlorophyllase is present during all stages of development, its activity is modulated by hormones that also affect leaf senescence and fruit ripening, such as kinetin and ethylene (Trebitsh et al., 1993; Jacob-Wilk et al., 1999).

The subcellular location of the third enzyme of Chl breakdown, Mg dechelatase (see Fig. 3), is not well established but preliminary information indicates that this constitutive enzyme is also located in the plastid envelope (Schellenberg and Matile, 1995; Vicentini et al., 1995b).

The key macrocycle cleavage enzymes, PaO, together with RCC reductase, both reside outside the thylakoid membrane. PaO has been attributed to the plastid envelope (Matile and Schellenberg, 1996), whereas RCC reductase is a soluble stroma protein (Rodoni et al., 1997a,b; Wüthrich et al., 2000). As for chlorophyllase, the expression of PaO and RCC reductase genes is not restricted to senescence (Wüthrich et al., 2000; Pružinská et al., 2003). Whereas RCC reductase is a constitutive enzyme, PaO activity is regulated in a senescence-specific way. Therefore, it has been proposed that PaO may be regulated post-transcriptionally, probably by protein modification (Pružinská et al., 2003).

In summary, most early reactions of Chl catabolism occur outside the thylakoid membrane and are, therefore, spatially separated from the primary substrate, Chl. This suggests that a carrier protein is necessary to establish contact between Chl and the early catabolic enzymes (Matile et al., 1996). While Pheide *a* (**6a**) and the Chlides (**3a** and **3b**) accumulate in the stay-green mutant Bf 993 of *F. pratensis* due to the absence of PaO, these dephytylated pigments do not occur when senescent leaves are treated with a protein biosynthesis inhibitor (Thomas et al., 1989). This suggests that a nuclear-encoded protein may be necessary for chlorophyllase to interact with Chl.

Chl catabolism includes catabolite export through the chloroplast membrane and import across the tonoplast into the vacuole (see Fig. 3). Both transport processes have been only partially characterized in isolated gerontoplasts of oilseed rape or barley leaves which not only synthesize FCCs but also excrete different FCCs, of currently unknown structures, across the plastid membrane in the presence of ATP (Matile et al., 1992). ATP is also required for import of Chl catabolites into the vacuole where the carrier on the tonoplast is a primary active ATPase (Hinder et al., 1996) of the multi-drug resistance-associated protein (MRP) type (Lu et al., 1998; Tommasini et al., 1998). These proteins , classified as ATP-binding cassette transporters, are implicated in the vacuolar import of a broad range of secondary compounds and xenobiotics (Martinoia et al., 2000). Thus, for example, AtMRP2 and AtMRP3 of *A. thaliana* can transport not only *Bn*-NCC-1 (**23**) but also glutathione S-conjugates into the vacuole (Lu et al., 1998; Tommasini et al., 1998). Unfortunately, the nature of the genuine tetrapyrrole substrate for vacuolar uptake has not been firmly established. Due to the low substrate specificity of such transport proteins (see above), both NCCs and FCCs might serve as substrates. It is noteworthy, however, that the catabolite carrier(s) of barley vacuoles had a particularly high affinity for a structurally unidentified FCC (Hinder et al., 1996) and contained small amounts of FCCs when isolated from senescent primary leaves (Matile et al., 1988). Consideration of the above-mentioned acid-catalyzed, non-enzymatic tautomerization of the pFCC (**11**-*epi*) to the corresponding NCC (**21**) (Oberhuber et al., 2003), suggests that transport of Chl catabolites across the tonoplast in vivo occurs at the level of FCCs which are then converted non-enzymatically to NCCs in the acidic milieu of the vacuole (see Fig. 3).

E. Chlorophyll Breakdown and the Nutrient Economy of Plants

Breakdown of Chl during plant senescence occurs within a major developmental program ultimately leading to the death of the respective tissues, such as leaves or fruits. Chl, together with lipids, proteins and nucleic acids, is degraded in large quantities during this process (Matile, 1992). Leaf senescence can be regarded as programmed cell death, but also serves in plants to re-mobilize nutrients to surviving organs (Smart, 1994). Major structural changes first occur within the chloroplasts: the contact between the grana stacks of the thylakoid membranes is loosened and, finally, the membranes disappear with concomitant loss of Chl and of soluble and membrane-bound proteins. Later in senescence, mitochondria and the nucleus are also affected before the cells finally die through the rupture of the tonoplast by autolysis (Thomas and Hilditch, 1987; Matile, 1992; Hörtensteiner and Feller, 2002).

The chloroplasts during senescence contribute substantially to nitrogen re-mobilization: about 75% of total cellular nitrogen is located within the chloroplasts (Makino and Osmond, 1991). The most abundant soluble chloroplast protein, Rubisco, and the Chl-binding apo-proteins of the thylakoid membranes are the main proteins lost during senescence (Matile, 1992). In contrast, the Chl molecule accounts for only about 2% of total cellular nitrogen (Peoples and Dalling, 1988). Polypeptide degradation of the light harvesting complex (LHC) II requires the simultaneous degradation of Chl: stay-green mutants of *F. pratensis* and *Phaseolus vulgaris,* which retain most of their Chl during senescence, cannot degrade LHCP II, whereas Rubisco is degraded as rapidly as in their respective wild types (Thomas and Hilditch, 1987); thus, Chl-binding in such pigment-proteins as LHCP II confers stability against proteolysis (White and Green, 1987).

While Chl catabolism is a prerequisite for the re-mobilization of the apo-proteins during plant senescence, the fact that Chl nitrogen is not released at the same time, but deposited as NCCs in the vacuole, raises the question: why do plants degrade Chl at all? There is striking evidence suggesting that Chl is transformed into colorless pigments to abolish its lethal photodynamic properties when it is released from the pigment-protein complexes (Kräutler et al., 1991; Hörtensteiner, 1999; Pružinská et al., 2003). Indeed, Chl catabolism in higher plants resembles, in many aspects, the stepwise detoxification of xenobiotics and herbicides (Kreuz et al., 1996).

III. Chlorophyll Breakdown and Chlorophyll Catabolites in Green Algae

It has been known since the 1960s that the green alga, *C. protothecoides,* when grown in nitrogen-deficient and glucose-rich medium, excretes red pigments (Oshio and Hase, 1969) which were structurally examined in the laboratory of Gossauer (Engel et al., 1991, 1996; Iturraspe et al., 1994; Curty et al., 1995; Gossauer and Engel, 1996; Curty and Engel, 1997). These red pigments were linear tetrapyrroles, similar to the colorless Chl catabolite, *Hv*-NCC-1 (**1**), resulting from oxygenolytic cleavage of the macrocycle at the 'northern' C5 bridge carbon. In contrast to the plant systems, the red catabolites were found to be derived from both Chls *a* (**2a**) and *b* (**2b**) (see Scheme 5; Iturraspe et al., 1994). Subsequent results indicated that the diacid **10** was the authentic product of enzymatic catabolism in *C. protothecoides* (Engel et al., 1996; Gossauer and Engel, 1996) rather than the monoacids, **31a** and **31b**, which were originally isolated and identified by Engel et al. (1991) as their respective monomethyl esters, **9a** and **9b** (see Schemes 5 and 13).

Labeling studies with $^{18}O_2$ followed by MS analysis of the excreted pigment as its ^{18}O-labeled methyl ester **9a**, clearly indicated incorporation of only one ^{18}O-atom into **9** (Curty et al., 1995). Analysis of a fragment confirmed that the ^{18}O-label was in the formyl group at the C5 carbon of Chl indicating that a monooxygenase cleaved the macrocycle in green alga (Curty et al., 1995): the direct substrate(s) and product(s) are not yet known. Deuterium labeling during degradation of the Chls in this green alga, showed highly stereo-selective attachment of one hydrogen atom (from water) at the 'eastern' C10 bridge carbon of the red isolate **9a**, indicating that this was an enzymatic step in the formation of the red catabolites (Curty and Engel, 1997). Based on the available chemical evidence, it was suggested that the formation of the RCCs in *C. protothecoides* arose from hydration of an epoxide intermediate and subsequent rearrangement (Engel et al., 1991, 1996; Curty and Engel, 1997). These, and related mechanistic considerations concerning Chl degradation in algae and higher plants, require further critical experiments. However, the structural resemblance of the algal catabolites and the plant RCC (**12**) and the similar oxygenolytic macrocycle cleavage mechanisms in higher plants (Hörtensteiner et al. 1998) and in *C. protothecoides* (Curty et al., 1995) indicate a clear biochemical relationship. Hence, the respective oxygenase of *C. protothecoides* and PaO of higher plants may display comparable catalytic properties. Notable differences concern the restriction of substrate specificity of the higher-plant enzyme to Chl *a* and its absolute requirement for a second enzyme, namely, RCC reductase (Hörtensteiner, 1999; Kräutler and Matile, 1999; Hörtensteiner and Kräutler, 2000): for this latter reason, the simple excretion of RCCs by the green alga is clearly not possible in vascular plants.

The excretion of another group of red bile pigments from senescent forms of a Chl *b*-less mutant of the green alga, *Chlamydomonas. reinhardtii,* has been reported (Doi et al., 1997). The UV/Vis-spectrum of the major pigment, tentatively named P535, displays absorbance maxima near 535, 385 and 275 nm, but these newly-found pigments have not yet

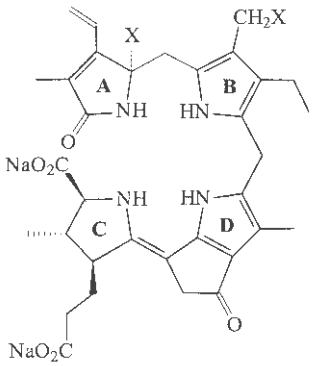

32: X = H
36: X = OH

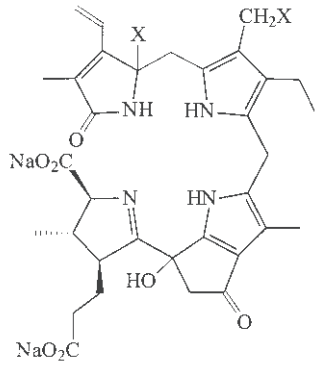

33: X = H
37: X = OH

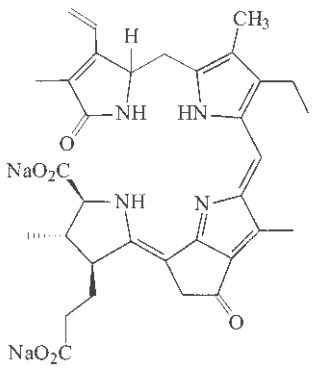

34

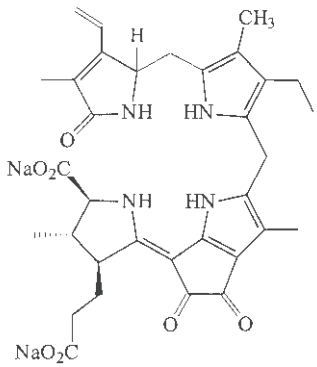

35

Scheme 14

been structurally identified. Accumulation of P535 required aerobic growth conditions and was prevented by inhibitors of cytoplasmic protein biosynthesis (Doi et al., 2001).

IV. Chlorophyll Catabolites from Marine Organisms

Photosynthetic organisms are widely distributed in the oceans. Relative to the information available on Chl catabolism in two green algae and in several higher plants, little is known about the fate of the Chls or bacteriochlorophylls from marine environments. One exception concerns a luciferin, isolated from the dinoflagellate, *Pyrocystis lunula,* which appeared structurally related to Chl (Dunlap et al., 1981). This colorless, luminescent compound, **32**, and two air oxidation products, **33** and **34**, were identified by spectroscopic and chemical degradation methods in the laboratory of Y. Kishi (see Scheme 14; Nakamura et al., 1989). Similar methods showed that the bioluminescent transformation of luciferin, **32**, by the dinoflagellate luciferase produced the oxidation product **35**. A related study of the light emitter from krill (*Euphasia pacifica*), assigned the structure of the related linear tetrapyrrole **36** which is also readily air oxidized to **37** (Nakamura et al., 1988). Both luminescent compounds (**32**, **36**) were identified as Chl derivatives, namely, 1,20-dioxo-1,20-seco-pyropheophorbides arising by an oxygenolytic cleavage at the 'western' C20 bridge carbons of their Chl precursor(s).

Further studies by Kishi and coworkers on the photooxygenolysis of the 20-methoxy-pyropheophorbide 38 have confirmed the tendency of some similarly

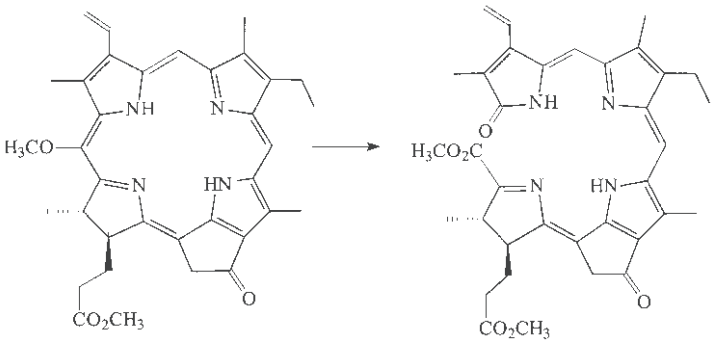

38 39

Scheme 15

substituted Pheides to undergo oxygenolytic cleavage of the chlorin macrocycle at the 'western' meso-position, between C20 and C1. This provides synthetic access to the 1,20-seco-pyropheophorbidate **39** (see Scheme 15; Topalov and Kishi, 2001).

Considering the absence of O_2 in deep sea water, an oxygenolytic mechanism may not be the dominant form of degradation of Chls from marine photosynthetic organisms.

V. Conclusions and Outlook

In the last fifteen years, the structures of many relevant Chl catabolites in higher plants were established thus gradually revealing the nature of plant Chl catabolism. The key step in the known degradation paths in green algae and in plants is an oxygenolytic cleavage of the porphinoid macrocycle. In higher plants this primary ring cleavage reaction specifically involves only Pheide *a*. In a series of (coupled) step(s) Chl breakdown rapidly reduces the chromophore of a photoactive and intensely colored chlorin to that of a colorless tetrapyrrole with de-conjugated hetero-cyclic rings. Nonfluorescent tetrapyrrolic Chl catabolites are considered to constitute the 'final' products of controlled Chl breakdown in senescent higher plants while in green algae the red pigments, which are excreted, are the final products of Chl catabolism. The degradation of the Chls in senescent leaves is reminiscent of the operation of detoxification processes.

The knowledge of the structure of key Chl catabolites and of some of the relevant higher plant enzymes involved in their formation now sets the stage for a series of further investigations in areas such as: (i) molecular regulation and cellular control of Chl breakdown, (ii) modes of action (and interaction) of the catabolic enzymes, (iii) possible physiological roles of tetrapyrrolic Chl breakdown products in senescent leaves, and (iv) the further general fate of the tetrapyrrolic remnants of the Chls in the senescent plant.

Note Added in Proof

Since preparation of this chapter, major progress has been achieved by the detailed analysis of Chl breakdown in the model plant *A. thaliana* (Pružinskà et al., 2005). It was shown that in contrast to the previous assumption of a posttranslational regulation of PAO, regulation mainly occurs at the level of *Pao* gene expression. Analysis of a *pao1* knockout mutant corroborates earlier work on maize (Pružinskà et al., 2003) and substantiates a key role for PAO in Chl breakdown.

Furthermore, this work includes the isolation and structural identification of colorless Chl catabolites. Thus, five different NCCs (*At*-NCC-1 to *At*-NCC-5) and three FCCs (*At*-FCC-1 to *At*-FCC-3) were identified during leaf senescence in *A. thaliana*; thereby *At*-NCC-1 and *At*-NCC-2, respectively, were identical to *Bn*-NCC-2 (**24**) and *Bn*-NCC-3 (**25**) of canola, and *At*-FCC-3 was identified with pFCC-1 (**11**). An NCC of intermediate polarity, named *At*-NCC-3, was discovered to be a constitutional isomer of *At*-NCC-2. In *At*-NCC-3, the substituents at C-8 and at C-7 were an ethyl group and a (functionalized) hydroxyl-methyl group, respectively. So far, the substituent at C-7 has always

been found to be a methyl group in all other NCCs, including *At*-NCC-2. The structure of *At*-NCC-3 thus indicated a deviation from the known path of Chl breakdown in *A. thaliana* (Müller, 2005). Rather large quantities of FCCs accumulated in *A. thaliana* during leaf senescence as compared to other systems analyzed so far. The identification of modified FCCs and structure elucidation of one of these corroborated an earlier suggestion that modifications as seen in the structures of NCCs occur at the FCC level.

Acknowledgments

We are indebted to Philippe Matile and his earlier coworkers, for their experimentally and intellectually fruitful collaboration, to Howard Thomas and his group for their important contributions to the problem of Chl breakdown. We thank specifically the members of the Chl group in Innsbruck: Michael Oberhuber, Joachim Berghold, Walter Mühlecker, Thomas Müller, Kathrin Breuker and Benjamin Gerlach, and in Bern: Adiana Pružinská and Iwona Anders for their enthusiastic work. We gratefully acknowledge financial support for this work from the Austrian National Science Foundation (FWF, projects No. P13503 and P16097) and from the Swiss National Science Foundation (project No. 31.63628).

References

Arabidopsis Genome Initiative (2000) Analysis of the genome sequence of the flowering plant *Arabidopsis thaliana*. Nature 408: 796–813

Bachmann A, Fernández-López J, Ginsburg S, Thomas H, Bouwcamp JC, Solomos T and Matile P (1994) *Stay-green* genotypes of *Phaseolus vulgaris* L.: Chloroplast proteins and chlorophyll catabolites during foliar senescence. New Phytol 126: 593–600

Beale SI and Cornejo J (1991) Biosynthesis of phycobilins. 15,16-Dihydrobiliverdin IXα is a partially reduced intermediate in the formation of phycobilins from biliverdin IXα. J Biol Chem 266: 22341–22345

Beale SI and Weinstein JD (1991) Biochemistry and regulation of photosynthetic pigment formation in plants and algae. In: Jordan, P M (ed) Biosynthesis of Tetrapyrroles, pp 155–235. Elsevier, Amsterdam

Berghold J, Breuker K, Oberhuber M, Hörtensteiner S and Kräutler B (2002) Chlorophyll breakdown in spinach: On the structure of five nonfluorescent chlorophyll catabolites. Photosynth Research 74: 109–119

Berghold J, Eichmüller C, Hörtensteiner S, Kräutler B (2004) Chlorophyll breadkown in tobacco: On the structure of two non-fluorescent chlorophyll catabolites. Chem Biodiv 1: 657–668

Bortlik K-H, Peisker C and Matile P (1990) A novel type of chlorophyll catabolite in senescent barley leaves. J Plant Physiol 136: 161–165

Brandis A, Vainstein A and Goldschmidt EE (1996) Distribution of chlorophyllase among components of chloroplast membranes in *Citrus sinensis* organs. Plant Physiol Biochem 34: 49–54

Brown SB, Houghton JD and Hendry GAF (1991) Chlorophyll breakdown. In: Scheer H (ed) Chlorophylls, pp 465–489. CRC Press, Boca Raton

Curty C and Engel N (1996) Detection, isolation and structure elucidation of a chlorophyll *a* catabolite from autumnal senescent leaves of *Cercidiphyllum japonicum*. Phytochemistry 42: 1531–1536

Curty C and Engel N (1997) Chlorophyll catabolism: High stereoselectivity in the last step of the primary ring cleaving process. Plant Physiol Biochem 35: 707–711

Curty C, Engel N and Gossauer A (1995) Evidence for a monooxygenase-catalyzed primary process in the catabolism of chlorophyll. FEBS Lett 364: 41–44

Doi M, Shima S, Egashira T, Nakamura K and Okayama S (1997) New bile pigment excreted by a *Chlamydomonas reinhardtii* mutant: A possible breakdown catabolite of chlorophyll *a*. J Plant Physiol 150: 504–508

Doi M, Inage T and Shioi Y (2001) Chlorophyll degradation in a *Chlamydomonas reinhardtii* mutant: An accumulation of pyropheophorbide *a* by anaerobiosis. Plant Cell Physiol 42: 469–474

Dunlap JC, Hastings JW and Shimomura O (1981) Dinoflagellate luciferin is structurally related to chlorophyll. FEBS Letters 135: 273–276

Engel N, Jenny TA, Mooser V and Gossauer A (1991) Chlorophyll catabolism in *Chlorella protothecoides.* Isolation and structure elucidation of a red bilin derivative. FEBS Lett 293: 131–133

Engel N, Curty C and Gossauer A (1996) Chlorophyll catabolism in *Chlorella protothecoides*. 8. Facts and artifacts. Plant Physiol Biochem 34: 77–83

Eschenmoser A (1988) Vitamin B_{12}: Experiments concerning the origin of its molecular structure. Angew Chem 100: 5–40; Angew Chem Int Ed Engl 27: 5–40

Falk H (1989) The Chemistry of Linear Oligopyrroles and Bile Pigments. Springer Verlag, Wien

Folley P and Engel N (1999) Chlorophyll *b* to chlorophyll *a* conversion precedes chlorophyll degradation in *Hordeum vulgare* L. J Biol Chem 274: 21811–21816

Frankenberg N, Mukougawa K, Kohchi T and Lagarias JC (2001) Functional genomic analysis of the HY2 family of ferredoxin-dependent bilin reductases from oxygenic photosynthetic organisms. Plant Cell 13: 965–978

Ginsburg S and Matile P (1993) Identification of catabolites of chlorophyll porphyrin in senescent rape cotyledons. Plant Physiol 102: 521–527

Ginsburg S, Schellenberg M and Matile P (1994) Cleavage of chlorophyll-porphyrin. Requirement for reduced ferredoxin and oxygen. Plant Physiol 105: 545–554

Gossauer A and Engel N (1996) Chlorophyll catabolism. Structures, mechanisms, conversions. J Photochem Photobiol B: Biol 32: 141–151

Gray J, Janick-Bruckner D, Bruckner B, Close PS and Johal GS (2002) Light-dependent death of maize *lls1* cells is mediated

by mature chloroplasts. Plant Physiol 130: 1894-1907
Greenberg JT, Guo A, Klessig DF and Ausubel FM (1994) Programmed cell death in plants: A pathogen-triggered response activated coordinately with multiple defense functions. Cell 77: 551–563
Hammond-Kosack K and Jones JDG (2001) Responses to plant pathogens. In: Buchanan BB, Gruissem W and Jones RL (eds) Biochemistry and Molecular Biology of Plants, pp 1102–1156. American Society of Plant Physiologists, Rockville
Hendry GAF, Houghton JD and Brown SB (1987) Chlorophyll degradation. A biological enigma. New Phytol 107: 255–302
Hinder B, Schellenberg M, Rodoni S, Ginsburg S, Vogt E, Martinoia E, Matile P and Hörtensteiner S (1996) How plants dispose of chlorophyll catabolites. Directly energized uptake of tetrapyrrolic breakdown products into isolated vacuoles. J Biol Chem 271: 27233–27236
Hörtensteiner S (1998) NCC malonyltransferase catalyses the final step of chlorophyll breakdown in rape (*Brassica napus*). Phytochemistry 49: 953–956
Hörtensteiner S (1999) Chlorophyll breakdown in higher plants and algae. Cell Mol Life Sci 56: 330–347
Hörtensteiner S and Feller U (2002) Nitrogen metabolism and remobilization during senescence. J Exp Bot 53: 927–937
Hörtensteiner S and Kräutler B (2000) Chlorophyll breakdown in oilseed rape. Photosynth Res 64: 137–146
Hörtensteiner S, Vicentini F and Matile P (1995) Chlorophyll breakdown in senescent cotyledons of rape, *Brassica napus L.*: Enzymatic cleavage of pheophorbide *a* in vitro. New Phytol 129: 237–246
Hörtensteiner S, Wüthrich KL, Matile P, Ongania K-H and Kräutler B (1998) The key step in chlorophyll breakdown in higher plants. Cleavage of pheophorbide *a* macrocycle by a monooxygenase. J Biol Chem 273: 15335–15339
Hörtensteiner S, Rodoni S, Schellenberg M, Vicentini F, Nandi OI, Qiu Y-L and Matile P (2000) Evolution of chlorophyll degradation: The significance of RCC reductase. Plant Biol 2: 63–67
Hynninen PH (1991) Chemistry of chlorophylls: Modifications. In: Scheer H (ed) Chlorophylls, pp 145–209. CRC Press, Boca Raton
Ito H and Tanaka A (1996) Determination of the activity of chlorophyll *b* to chlorophyll *a* conversion during greening of etiolated cucumber cotyledons by using pyrochlorophyllide *b*. Plant Physiol Biochem 34: 35–40
Ito H, Tanaka Y, Tsuji H and Tanaka A (1993) Conversion of chlorophyll *b* to chlorophyll *a* by isolated cucumber etioplasts. Arch Biochem Biophys 306: 148–151
Iturraspe J and Gossauer A (1992) A biomimetic partial synthesis of the red chlorophyll-*a* catabolite from *Chlorella protothecoides*. Tetrahedron 48: 6807–6812
Iturraspe J, Engel N and Gossauer A (1994) Chlorophyll catabolism. Isolation and structure elucidation of chlorophyll *b* catabolites in *Chlorella protothecoides*. Phytochemistry 35: 1387–1390
Iturraspe J, Moyano N and Frydman B (1995) A new 5-formylbilinone as the major chlorophyll *a* catabolite in tree senescent leaves. J Org Chem 60: 6664–6665
Jakob-Wilk D, Holland D, Goldschmidt EE, Riov J and Eyal Y (1999) Chlorophyll breakdown by chlorophyllase: Isolation and functional expression of the *Chlase1* gene from ethylene-treated *Citrus* fruit and its regulation during development. Plant J 20: 653–661
Kräutler B (2002) Unravelling chlorophyll catabolism in higher plants. Biochem Soc Trans 30: 625–630
Kräutler B (2003) Chlorophyll breakdown and chlorophyll catabolites. In: Kadish K M, Smith K M and Guilard R (eds) The Porphyrin Handbook, Vol. 11, pp. 183–209. Elsevier Science
Kräutler B and Matile P (1999) Solving the riddle of chlorophyll breakdown. Acc Chem Res 32: 35–43
Kräutler B, Jaun B, Bortlik K-H, Schellenberg M and Matile P (1991) On the enigma of chlorophyll degradation: The constitution of a secoporphinoid catabolite. Angew Chem Int Ed Engl 30: 1315–1318
Kräutler B, Jaun B, Amrein W, Bortlik K-H, Schellenberg M and Matile P (1992) Breakdown of chlorophyll: Constitution of a secoporphinoid chlorophyll catabolite isolated from senescent barley leaves. Plant Physiol Biochem 30: 333–346
Kräutler B, Mühlecker W, Anderl M and Gerlach B (1997) Breakdown of chlorophyll: Partial synthesis of a putative intermediary catabolite. Helv Chim Acta 80: 1355–1362
Kreuz K, Tommasini R and Martinoia E (1996) Old enzymes for a new job. Herbicide detoxification in plants. Plant Physiol 111: 349–353
Langmeier M, Ginsburg S and Matile P (1993) Chlorophyll breakdown in senescent leaves: Demonstration of Mg-dechelatase activity. Physiol Plant 89: 347–353
Lippard SJ and Berg JM (1994) Oxygen-atom transfer reactions: Fe. In: Lippard SJ and Berg JM, Principles of Bioinorganic Chemistry, pp 302–318. University Science Books, Mill Valley
Llewellyn CA, Mantoura RFC and Brereton G (1990) Products of chlorophyll photodegradation. 2. Structural identification. Photochem Photobiol 52: 1043–1047
Losey FG and Engel N (2001) Isolation and characterization of a urobilinogenoidic chlorophyll catabolite from *Hordeum vulgare* L. J Biol Chem 276: 27233–27236
Lu Y-P, Li Z-S, Drozdowicz Y-M, Hörtensteiner S, Martinoia E and Rea PA (1998) AtMRP2, an *Arabidopsis* ATP binding cassette transporter able to transport glutathione *S*-conjugates and chlorophyll catabolites: Functional comparisons with AtMRP1. Plant Cell 10: 267–282
Mach JM, Castillo AR, Hoogstraten R and Greenberg JT (2001) The *Arabidopsis*-accelerated cell death gene ACD2 encodes red chlorophyll catabolite reductase and suppresses the spread of disease symptoms. Proc Natl Acad Sci USA 98: 771–776
Makino A and Osmond B (1991) Effect of nitrogen nutrition on nitrogen partitioning between chloroplasts and mitochondria in pea and wheat. Plant Physiol 96: 355–362
Martinoia E, Klein M, Geisler M, Sánchez-Fernández R and Rea PA (2000) Vacuolar transport of secondary metabolites and xenobiotics. In: Robinson DG and Rogers JC (eds) Vacuolar Compartments. Annual Plant Reviews, Vol 5, pp 221–253. Sheffield Academic Press, Sheffield
Matile P (1987) Seneszenz bei Pflanzen und ihre Bedeutung für den Stickstoffhaushalt. Chimia 41: 376–381
Matile P (1992) Chloroplast senescence. In: Baker NR and Thomas H (eds) Crop Photosynthesis: Spatial and Temporal Determinants, pp 413–440. Elsevier Science Publishers, Amsterdam
Matile P (1997) The vacuole and cell senescence. In: Callow JA (ed) Advances in Botanical Research, Vol 25, pp 87–112. Academic Press, New York

Matile P and Schellenberg M (1996) The cleavage of pheophorbide *a* is located in the envelope of barley gerontoplasts. Plant Physiol Biochem 34: 55–59

Matile P, Ginsburg S, Schellenberg M and Thomas H (1987) Catabolites of chlorophyll in senescent leaves. J Plant Physiol 129: 219–228

Matile P, Ginsburg S, Schellenberg M and Thomas H (1988) Catabolites of chlorophyll in senescing barley leaves are localized in the vacuoles of mesophyll cells. Proc Natl Acad Sci USA 85: 9529–9532

Matile P, Schellenberg M and Peisker C (1992) Production and release of a chlorophyll catabolite in isolated senescent chloroplasts. Planta 187: 230–235

Matile P, Hörtensteiner S, Thomas H and Kräutler B (1996) Chlorophyll breakdown in senescent leaves. Plant Physiol 112: 1403–1409

Matile P, Schellenberg M and Vicentini F (1997) Localization of chlorophyllase in the chloroplast envelope. Planta 201: 96–99

Matile P, Hörtensteiner S, Thomas H (1999) Chlorophyll degradation. Annu Rev Plant Physiol Plant Mol Biol 50: 67–95

McFeeters RF (1975) Substrate specificity of chlorophyllase. Plant Physiol 55: 377–381

Mendel G (1865) Versuche über Pflanzenhybriden. Verh Naturf Ver 4: 3–47

Moss GP (1987) Nomenclature of Tetrapyrroles. Pure Appl Chem 59: 779–832

Mühlecker W and Kräutler B (1996) Breakdown of chlorophyll: Constitution of nonfluorescing chlorophyll-catabolites from senescent cotyledons of the dicot rape. Plant Physiol Biochem 34: 61–75

Mühlecker W, Kräutler B, Ginsburg S and Matile P (1993) Breakdown of chlorophyll: The constitution of a secoporphinoid chlorophyll catabolite from senescent rape leaves. Helv Chim Acta 76: 2976–2980

Mühlecker W, Ongania K-H, Kräutler B, Matile P and Hörtensteiner S (1997) Tracking down chlorophyll breakdown in plants: Elucidation of the constitution of a 'fluorescent' chlorophyll catabolite. Angew Chem Int Ed Engl 36: 401–404

Mühlecker W, Kräutler B, Moser D, Matile P and Hörtensteiner S (2000) Breakdown of chlorophyll: A fluorescent chlorophyll catabolite from sweet pepper (*Capsicum annuum*). Helv Chim Acta 83: 278–286

Müller T, Moser S, Ongania K-H, Hörtensteiner S and Kräutler B (2005) A divergent path of chlorophyll breakdown in the model plant *Arabidopsis thaliana*. ChemBioChem 7: 40–42

Nakamura H, Musicki B, Kishi Y and Shimomura O (1988) Structure of the light emitter in krill (*Euphausia pacifica*) bioluminescence. J Am Chem Soc 110: 2683–2685

Nakamura H, Kishi Y, Shimomura O, Morse D and Hastings JW (1989) Structure of dinoflagellate luciferin and its enzymatic and nonenzymatic air-oxidation products. J Am Chem Soc 111: 7607–7611

Oberhuber M and Kräutler B (2002) Breakdown of chlorophyll: Electrochemical bilin reduction provides synthetic access to fluorescent chlorophyll catabolites. Chem Bio Chem 3: 104–107

Oberhuber M, Berghold J, Mühlecker W, Hörtensteiner S and Kräutler B (2001) Chlorophyll breakdown — on a nonfluorescent chlorophyll catabolite from spinach. Helv Chim Acta 84: 2615–2627

Oberhuber M, Berghold J, Breuker K, Hörtensteiner S and Kräutler B (2003) Breakdown of chlorophyll: A nonenzymatic reaction accounts for the formation of the colorless 'nonfluorescent' chlorophyll catabolites. Proc. Natl Acad Sci USA 74: 6910–6915

Ohtsuka T, Ito H and Tanaka A (1997) Conversion of chlorophyll *b* to chlorophyll *a* and the assembly of chlorophyll with apoproteins by isolated chloroplasts. Plant Physiol 113: 137–147

Oshio Y and Hase E (1969) Studies on red pigments excreted by cells of *Chlorella protothecoides* during the process of bleaching induced by glucose or acetate. I. Chemical properties of the red pigments. Plant Cell Physiol 10: 41–49

Paulsen H, Finkenzeller B and Kühnlein N (1993) Pigments induce folding of light-harvesting chlorophyll *a*/*b*-binding protein. Eur J Biochem 215: 809–816

Peisker C, Thomas H, Keller F and Matile P (1990) Radiolabelling of chlorophyll for studies on catabolism. J Plant Physiol 136: 544–549

Peoples MB and Dalling MJ (1988) The interplay between proteolysis and amino acid metabolism during senescence and nitrogen allocation. In: Noodén LD and Leopold AC (eds) Senescence and Aging in Plants, pp 181–217. Academic Press, San Diego

Porra RJ, Schäfer W, Cmiel E, Katheder I and Scheer H (1994) The derivation of the formyl-group oxygen of chlorophyll *b* in higher plants from molecular oxygen. Achievement of high enrichment of the 7-formyl-group oxygen from $^{18}O_2$ in greening maize leaves. Eur J Biochem 219: 671–679

Pružinská A, Tanner G, Anders I, Roca M and Hörtensteiner S (2003) Chlorophyll breakdown: Pheophorbide *a* oxygenase is a Rieske-type iron-sulfur protein, encoded by the *accelerated cell death 1* gene. Proc Natl Acad Sci USA 100: 15259–15264

Pružinskà A, Tanner G, Aubry S, Anders I, Moser S, Müller T, Ongania K-H, Kräutler B, Youn J-Y, Liljegren SJ and Hörtensteiner S (2005) Chlorophyll breakdown in senescent *Arabidopsis* leaves. Characterization of chlorophyll catabolites and of chlorophyll catabolic enzymes involved in the degreening reaction. Plant Physiol 139: 52–63

Rodoni S, Mühlecker W, Anderl M, Kräutler B, Moser D, Thomas H, Matile P and Hörtensteiner S (1997a) Chlorophyll breakdown in senescent chloroplasts. Cleavage of pheophorbide *a* in two enzymic steps. Plant Physiol 115: 669–676

Rodoni S, Vicentini F, Schellenberg M, Matile P and Hörtensteiner S (1997b) Partial purification and characterization of red chlorophyll catabolite reductase, a stroma protein involved in chlorophyll breakdown. Plant Physiol 115: 677–682

Rüdiger W (1997) Chlorophyll metabolism: From outer space down to the molecular level. Phytochemistry 46: 1151–1167

Schellenberg M and Matile P (1995) Association of components of the chlorophyll catabolic system with pigment-protein complexes from solubilized chloroplast membranes. J Plant Physiol 146: 604–608

Schellenberg M, Matile P and Thomas H (1990) Breakdown of chlorophyll in chloroplasts of senescent barley leaves depends on ATP. J Plant Physiol 136: 564–568

Schellenberg M, Matile P and Thomas H (1993) Production of a presumptive chlorophyll catabolite in vitro: Requirement for reduced ferredoxin. Planta 191: 417–420

Scheumann V, Ito H, Tanaka A, Schoch S and Rüdiger W (1996) Substrate specificity of chlorophyll(ide) *b* reductase in etioplasts of barley (*Hordeum vulgare*). Eur J Biochem 242: 163–170

Scheumann V, Schoch S and Rüdiger W (1999) Chlorophyll *b* reduction during senescence of barley seedlings. Planta 209: 364–370

Schoch S, Scheer H, Schiff JA, Rüdiger W and Siegelman HW (1981) Pyropheophytin *a* accompanies pheophytin *a* in darkened light grown cells of *Euglena*. Z Naturforsch 36c: 827–833

Shioi Y, Tatsumi Y and Shimokawa K (1991) Enzymatic degradation of chlorophyll in *Chenopodium album*. Plant Cell Physiol 32: 87–93

Shioi Y, Tomita N, Tsuchiya T and Takamiya K (1996a) Conversion of chlorophyllide to pheophorbide by Mg-dechelating substance in extracts of *Chenopodium album*. Plant Physiol Biochem 34: 41–47

Shioi Y, Watanabe K and Takamiya K (1996b) Enzymatic conversion of pheophorbide *a* to a precursor of pyropheophorbide *a* in leaves of *Chenopodium album*. Plant Cell Physiol 37: 1143–1149

Smart CM (1994) Gene expression during leaf senescence. New Phytol 126: 419–448

Stoll A (1912) Über Chlorophyllase und die Chlorophyllide. Thesis, ETH Zürich

Suzuki Y and Shioi Y (1999) Detection of chlorophyll breakdown products in the senescent leaves of higher plants. Plant Cell Physiol 40: 909–915

Takamiya K, Tsuchiya T and Ohta H (2000) Degradation pathway of chlorophyll in higher plants. What gene cloning has brought about. Trends Plant Sci 5: 426–431

Tanaka A, Ito H, Tanaka R, Tanaka NK, Yoshida K and Okada K (1998) Chlorophyll *a* oxygenase (*CAO*) is involved in chlorophyll *b* formation from chlorophyll *a*. Proc Natl Acad Sci USA 95: 12719–12723

Thomas H (1987) Foliar senescence mutants and other genetic variants. In: Thomas H and Grierson D (eds) Developmental Mutants in Higher Plants, pp 245–265. Cambridge University Press, Cambridge

Thomas H and Hilditch P (1987) Metabolism of thylakoid membrane proteins during foliar senescence. In: Thomson WW, Nothnagel EA and Huffaker RC (eds) Plant Senescence: Its Biochemistry and Physiology, pp 114–122. The American Society of Plant Physiologists, Rockville

Thomas H, Bortlik K-H, Rentsch D, Schellenberg M and Matile P (1989) Catabolism of chlorophyll in vivo: Significance of polar chlorophyll catabolites in a non-yellowing senescence mutant of *Festuca pratensis* Huds. New Phytol 111: 3–8

Thomas H, Schellenberg M, Vicentini F and Matile P (1996) Gregor Mendel's green and yellow pea seeds. Bot Acta 109: 3–4

Tommasini R, Vogt E, Fromenteau M, Hörtensteiner S, Matile P, Amrhein N and Martinoia E (1998) An ABC transporter of *Arabidopsis thaliana* has both glutathione-conjugate and chlorophyll catabolite transport activity. Plant J 13: 773–780

Topalov G and Kishi Y (2001) Chlorophyll catabolism leading to the skeleton of dinoflagellate and krill luciferins: Hypothesis and model studies. Angew Chem Int Ed Engl 40: 3892–3894

Trebitsh T, Goldschmidt EE and Riov J (1993) Ethylene induces *de novo* synthesis of chlorophyllase, a chlorophyll degrading enzyme, in *Citrus* fruit peel. Proc Natl Acad Sci USA 90: 9441–9445

Tsuchiya T, Ohta H, Masuda T, Mikami B, Kita N, Shioi Y and Takamiya K (1997) Purification and characterization of two isozymes of chlorophyllase from mature leaves of *Chenopodium album*. Plant Cell Physiol 38: 1026–1031

Tsuchiya T, Ohta H, Okawa K, Iwamatsu A, Shimada H, Masuda T and Takamiya K (1999) Cloning of chlorophyllase, key enzyme in chlorophyll degradation: Finding of a lipase motif and induction by methyl jasmonate. Proc Natl Acad Sci USA 96: 15362–15367

Vicentini F, Hörtensteiner S, Schellenberg M, Thomas H and Matile P (1995a) Chlorophyll breakdown in senescent leaves: Identification of the biochemical lesion in a *stay-green* genotype of *Festuca pratensis* Huds. New Phytol 129: 247–252

Vicentini F, Iten F and Matile P (1995b) Development of an assay for Mg-dechelatase of oilseed rape cotyledons, using chlorophyllin as the substrate. Physiol Plant 94: 57–63

White MJ and Green BR (1987) Polypeptides belonging to each of the three major chlorophyll *a*+*b* protein complexes are present in a chlorophyll-*b*-less barley mutant. Eur J Biochem 165: 531–535

Woodward RB and Skaric VJ (1961) A new aspect of the chemistry of chlorins. J Am Chem Soc 83: 4676–4678

Wüthrich KL, Bovet L, Hunziker PE, Donnison IS and Hörtensteiner S (2000) Molecular cloning, functional expression and characterization of RCC reductase involved in chlorophyll catabolism. Plant J 21: 189–198

Ziegler R, Blaheta A, Guha N and Schönegge B (1988) Enzymatic formation of pheophorbide and pyropheophorbide during chlorophyll degradation in a mutant of *Chlorella fusca* Shiria et Kraus. J Plant Physiol 132: 327–332